

See discussions, stats, and author profiles for this publication at: <https://www.researchgate.net/publication/384521257>

# Unlocking the potential of electric and hybrid tractors via sensitivity and techno-economic analysis

Article in Applied Energy · September 2024

DOI: 10.1016/j.apenergy.2024.124545

---

CITATIONS

4

5 authors, including:



Ricardo Castro  
University of California, Merced  
106 PUBLICATIONS 1,605 CITATIONS

[SEE PROFILE](#)

---

READS

118

Reza Ehsani

University of California, Merced

255 PUBLICATIONS 9,389 CITATIONS

[SEE PROFILE](#)



Stavros Vougioukas  
University of California, Davis  
173 PUBLICATIONS 2,928 CITATIONS

[SEE PROFILE](#)



Peng Wei  
University of California, Davis  
20 PUBLICATIONS 125 CITATIONS

[SEE PROFILE](#)

# Unlocking the Potential of Electric and Hybrid Tractors via Sensitivity and Techno-Economic Analysis

Dilawer Ali\*, Ricardo de Castro\*, Reza Ehsani\*, Stavros Vougioukas†, Peng Wei†

\*Department of Mechanical Engineering, University of California, Merced, CA, USA

†Department of Biological and Agricultural Engineering, Davis, CA, USA

**Abstract**—The majority of agricultural vehicles in use today still rely on diesel-based propulsion, a major source of air pollution. Electrification is seen as a potential solution for decarbonizing these off-road vehicles but is hampered by higher upfront costs in energy storage and charging infrastructure. To better quantify these barriers, this paper proposes a techno-economic tool that can assist farmers in evaluating the total costs of ownership of electric and hybrid tractors. A pragmatic simulation model of the tractor is developed to predict the annual energy/fuel consumption and NOx emissions, while an economic model estimates the total acquisition, operation, and maintenance costs. For managing the energy in hybrid tractors, a new power split strategy based on model predictive control is developed, allowing the designer to balance energy efficiency and NOx emissions, while taking into account operational constraints of the electric powertrain. Additionally, we propose novel decision maps that allow farmers to quickly identify operating regions (in term of average load and yearly working time) where the deployment of electric/hybrid tractors is economically viable. To account for variability in the tractor's operational conditions, we conduct both a deterministic sensitivity analysis with multi-parameter variation and a stochastic analysis of the total cost of ownership. The tool is validated with different mission profiles based on data from a California farm. The results show that, compared to diesel powertrains, electric tractors are more cost-effective for light-duty farming activities (engine loads less than 20%). On the other hand, hybrid powertrains are more economical for medium-duty tasks, where engine loads range from 20% to 60%.

## I. INTRODUCTION

Off-road agricultural vehicles, such as tractors, are crucial in providing power to a wide range of farming tasks, tillage, spraying, and harvesting. These off-road vehicles are a significant source of global greenhouse gas emissions [1]. Because of the world's population growth, the number of agricultural tractors has been steadily increasing over the years to meet the higher demand for food production. Currently, there are more than 4 million tractors in the USA alone [2], almost all of them powered by diesel engines. There is a critical need to de-carbonize agriculture and promote sustainable and clean agricultural vehicles. Motivated by these environmental concerns, regulations are being introduced to accelerate the transition toward zero-emission vehicles. For example, California has recently approved regulations to promote off-road

The authors would like to thank CITRIS (Center for Information Technology Research in the Interest of Society) for the financial support that enabled this research.

zero-emission vehicles by 2045 [3]. To meet these emerging regulations, manufacturers of off-road vehicles are considering electric drivelines. For example, Monarch [4] and Soletrac [5] recently introduced their first electric tractors in the American market. These vehicles have zero local emissions and can be directly charged from on-site renewable energy sources such as photovoltaic or bio-gas power plants, which are increasingly available in today's farms [6].

Despite their environmental advantages, battery-based electric tractors are more costly to acquire than diesel counterparts and face significant power and energy limitations. Charging an electric tractor is also a growing concern, given the limited electric infrastructure available in rural areas. Upgrades in the local grid infrastructure might be necessary, further increasing costs. Because of such challenges, transitioning from today's diesel-dominated agricultural machines to tomorrow's zero-emission tractors will be a long journey.

Tractor electrification can be performed at either i) the *auxiliary-load level* or ii) the *powertrain level*. In the first case, electric motors are used to drive high-power loads located onboard the tractor and/or in the implement. Examples of such loads include cooling fans [7], HVAC (heating, ventilation, and air conditioning) compressors, pumps [8], and augers [9]. These auxiliary loads can be powered by a small battery and a generator connected to the tractor's internal combustion engine (ICE). The main advantage of this approach is the ability to independently control the speed of each auxiliary load, allowing the ICE to operate in regions of high energy efficiency and reducing fuel consumption [8]. However, this approach only provides partial electrification, leading to partial fuel and environmental benefits.

Within *powertrain-level* electrification, we have battery- [8], hybrid- [10], [11] and fuel cell- [12] based tractors. Battery-based electric tractors are an attractive short-term option, which can benefit from improved performance, safety, and affordability of automotive batteries over the last decade [13]. The first electric tractors on the market, such as [4] and [5], rely on Lithium-ion batteries and appear well suited to support light-duty farming tasks. However, given batteries' limited energy density and high purchase price, concerns exist about scaling battery-based tractors to medium- and heavy-duty tasks. Hybrid tractors, which combine an electric motor and a diesel engine in the same powertrain [10], [11], are another potential short-term option for electrification. They provide

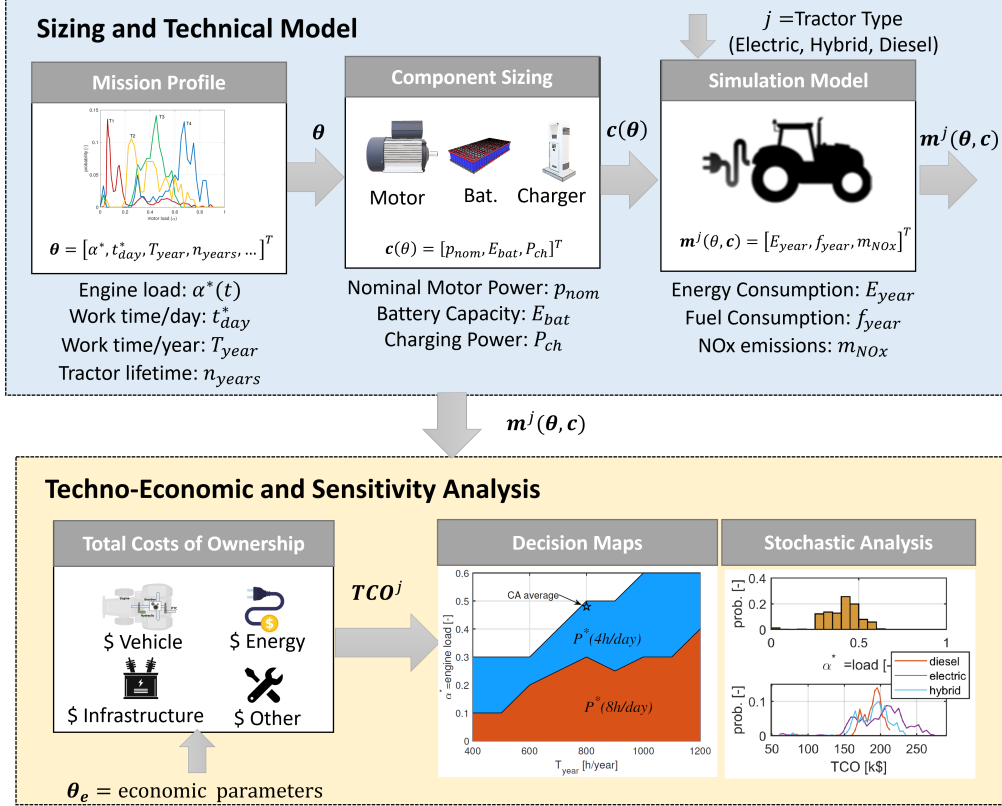


Fig. 1. Overview of the techno-economic process employed to compute tractors' total costs of ownership (TCO).

two key advantages: i) the diesel generator can support heavy-duty operations without requiring frequent stops for battery recharging; ii) the usage of an electric motor can be leveraged to downsize the diesel engine and shift its operation to points with higher energy efficiency [14]. However, this approach complicates the design and operation of the powertrain since two types of energy storage and conversion are needed. It also generates local emissions, which is not ideal from an environmental perspective. In the long run, fuel cells represent an attractive energy storage option for heavy-duty tractors given their high energy density [15], [16]. Still, they also face their own set of challenges related to the generation and distribution of hydrogen for refueling [12].

This work focuses on evaluating the economic benefits of electric and hybrid tractors as an alternative to conventional diesel-based tractors. We use the total costs of ownership (TCO) as the main evaluation criteria, which is also a critical metric to persuade farmers to acquire electrified tractors. TCO comparisons between diesel and electric powertrains have been widely performed in the last decade for light, medium, and heavy-duty on-road vehicles [17], [18]. The TCO analysis of off-road electric vehicles, such as tractors, is gaining increasing interest as the vehicle electrification effort expands into off-road domains. Our analysis also consider emissions of nitrogen oxides (NOx), which is one of the primary pollutants affecting the air quality in California, particularly the San Joaquin Valley [19].

The TCO of conventional powertrains has been extensively studied in the context of farm operations [20], [21]. For

example, the American Society of Agricultural and Biological Engineers (ASABE) published the standard EP496.2 [22] that guides farmers in calculating the TCO of gasoline and diesel tractors, accounting for acquisition and operating costs such as repairs, fuel, and labor. More recently, the TCO of electrified tractors has begun to receive attention in the literature [23]–[25]. These studies typically involve detailed simulation models of the tractor's powertrain, which enable more accurate assessments of battery discharge profiles and the operating time per charge—a critical factor given the range limitations of battery-based tractors [12]. In the case of hybrid tractors, TCO analysis must also consider the sizing of the engine and electric motor, along with the energy management strategy used to distribute power between the two propulsion systems. Heuristic strategies, like rule-based control [11], [14], are common because they are straightforward to implement and computationally inexpensive. Another significant challenge in TCO analysis is accounting for operating and cost uncertainties. Most studies incorporate deterministic sensitivity analyses, where parameters such as battery acquisition costs [23] and future fuel prices [11] are varied to assess their impact on overall techno-economic metrics.

This work provides two main contributions to the TCO analysis of electrified agricultural tractors.

First, we perform a systematic techno-economic benchmarking of electric, hybrid and diesel powertrains. This benchmarking takes into account a wide variety of mission profiles based on experimental data that we collected from multiple tractors in a California farm.

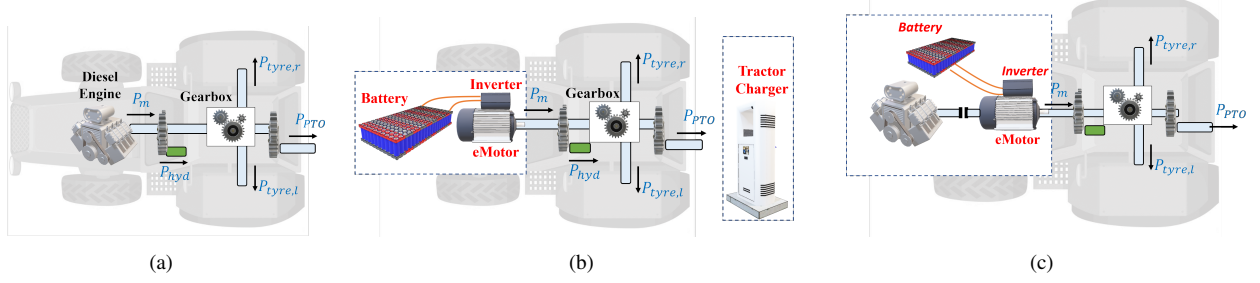


Fig. 2. Block diagram of the powertrains considered in this work: a) diesel, b) electric, and c) hybrid.

The energy management of the hybrid powertrain utilizes a model predictive control (MPC) framework [26]. This allows the designer to optimize energy efficiency and NOx emissions while considering multiple power and energy constraints in the battery. This approach contrasts with previous research on the TCO of hybrid tractors, which primarily focused on rule-based approaches [10], [11], [27]. While these methods are easier to apply, they typically provide only sub-optimal performance. It is worth noting that MPC has recently been applied to the velocity control of hybrid tractors, as discussed by [28] and [29]. However, this prior MPC research does not integrate a detailed economic model of the electric tractor, nor does it include a TCO analysis, which is the main focus of our work.

The second contribution introduces a novel decision map that projects the TCO results into a low-dimensional parameter space defined by key mission profile parameters, such as average tractor load and annual operating hours (see Fig. 1). These maps serve as a practical tool for quickly identifying the operating conditions under which deploying electric tractors becomes economically viable. They also facilitate the application of sensitivity analysis methods [30] to the TCO of electrified tractors, allowing us to visualize the TCO impact of varying up to three model parameters simultaneously. This represents an improvement over previous TCO studies on electrified tractors, which limited sensitivity analyses to one-at-a-time [23], [24], [31] and two-at-a-time [11] approaches. Additionally, we perform a stochastic TCO analysis that accounts for variability in the tractor's operational load, a key source of uncertainty. This approach contrasts with previous studies on the TCO of electrified tractors, such as those by [11] and [15], [27], which primarily relied on deterministic evaluation frameworks with limited capacity to address model uncertainties.

A preliminary version of this work was presented at [32]. It is extended here with additional powertrain variants (hybrid), a detailed description of the methodology, and an expanded (sensitivity) analysis of the TCO model.

## II. OVERVIEW OF METHODOLOGY

Fig. 1 provides an overview of the process employed to compute the TCO of tractors. This process can be divided into four main steps. The first step defines the operational requirements and mission profile ( $\theta$ ) for the tractor, including work intensity (i.e., engine load), operating hours per day and year, and the tractor's expected lifetime. This information

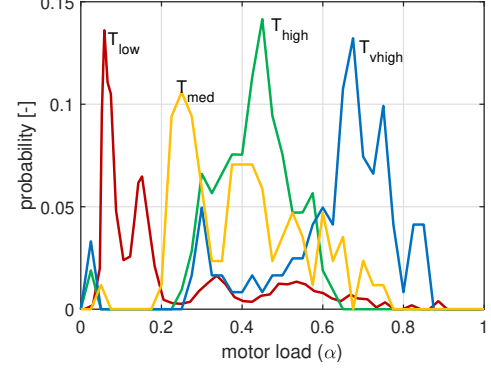


Fig. 3. Probability distribution function of the motor load  $\alpha$  for the tractors ( $T_{low}$ ,  $T_{med}$ ,  $T_{high}$ ,  $T_{vhigh}$ ) .

is then used in the second step to size the tractor components ( $\mathbf{c}(\theta)$ ), e.g., the capacity of the battery and charging power. The third step predicts the operation of the tractor using a numerical simulation model, which is particularly important to estimate the yearly energy ( $E_{year}$ ) and fuel ( $f_{year}$ ) consumption, as well as NOx emissions of the tractor ( $m_{NOx}$ ). Three simulation models  $\mathbf{m}^j$  are considered in this work:  $j \in \{\text{electric, hybrid, diesel}\}$ . The fourth and last step evaluates the TCO, including purchase, infrastructure, energy, and maintenance costs. The overall TCO computation is dependent on the powertrain type ( $j$ ), mission profile ( $\theta$ ), component sizing ( $\mathbf{c}$ ), simulation model ( $\mathbf{m}^j$ ), and parameters of the economic model ( $\theta_e$ ):

$$TCO^j(\theta, \mathbf{c}, \mathbf{m}^j, \theta_e) \quad (1)$$

This section provides an overview of technical methodology to determine  $\theta$ ,  $\mathbf{c}$  and  $\mathbf{m}^j$ , while the next section describes the TCO model and its economic parameters ( $\theta_e$ ).

### A. Powertrain Type ( $j$ )

Three types of tractor drivetrains are considered in this work: i) diesel, ii) fully electric, and iii) hybrid configuration that combines electric and diesel engines (see Fig. 2c). Regarding the hybrid powertrain, we assumed a parallel hybrid configuration, where the electric motor is inserted between the diesel engine's clutch and the mechanical transmission [13]. The main benefit of this configuration is low complexity since the electric motor can support the diesel engine and quickly charge the battery.

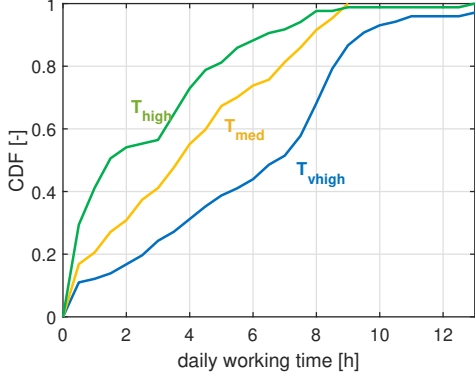


Fig. 4. Cumulative distribution function for the daily working time for the Merced's small fleet of tractors ( $T_{med}$ ,  $T_{high}$ ,  $T_{vhigh}$ )

TABLE I  
OVERVIEW OF TRACTORS FOR DATA COLLECTION ( NOTE THAT TRACTORS ARE RANKED BASED ON AVERAGE LOAD)

| Label       | Tractor Model       | Avg.<br>Load | Avg.<br>$t_{day}^{(1)}$ | Usage          |
|-------------|---------------------|--------------|-------------------------|----------------|
| $T_{low}$   | Custom tractor [11] | 0.14         | -                       | Orchards       |
| $T_{med}$   | John Deere 6155M    | 0.38         | 3.7                     | Dairy/Corn/Hay |
| $T_{high}$  | John Deere 7R210    | 0.43         | 1.5                     | Dairy/Corn/Hay |
| $T_{vhigh}$ | John Deere 9570R    | 0.65         | 6.8                     | Dairy/Corn/Hay |

<sup>(1)</sup> in h/day

To simplify comparison, all tractor types are assumed to employ the same mechanical transmission, e.g., a rear-wheel drive system connected to a gearbox with multiple ratios [33]. The drivetrain is responsible for delivering power to a wide range of loads. In addition to the tractive power provided to the tractor's tires ( $P_{tyre,r}$ ,  $P_{tyre,l}$  in Fig. 2), the motor supplies power to the hydraulic sub-system ( $P_{hyd}$ ), e.g., to raise and lower the implement, and to the power takeoff (PTO) unit ( $P_{PTO}$ ) that transmits power to the implement, and also electric loads, e.g., lights, cabin cooling/heating, etc. In practice, it is difficult to collect the power profiles of the individual loads of the tractor. To overcome this difficulty, we focus on the total power requested by the motor ( $P_m$ ), which aggregates the contribution of all types of loads.

In this work, we also assume that the electrified tractor preserves the mechanical interfaces of the PTO found in today's tractors [33]. This ensures compatibility with existing implements, allowing farmers to adopt the electric tractor without needing to replace their current implements.

### B. Mission Profile ( $\theta$ )

Tractors are considered a "universal" farming tool, capable of supporting a wide range of tasks, including tillage, fertilizing application, weeding, harvesting, etc [33]. As a result, their mission profile is highly dependent on the type of task and implements, which vary from farm to farm. To facilitate this characterization of the mission profile of the tractor, we employ the normalized load ( $\alpha$ ), which is defined as the ratio

of the motor power ( $P_m$ ) over the tractor's nominal power ( $P_{nom}$ ):

$$\alpha(t) = \frac{P_m(t)}{P_{nom}} \quad (2)$$

where  $\alpha(t)$  is the instantaneous (power) load. Fig. 3 represents the probability density function of the motor load for four different tractors considered in this study. The first tractor ( $T_{low}$ ) data is based on orchard tasks [11].

The data of the remaining three tractors ( $T_{med}$ ,  $T_{high}$ ,  $T_{vhigh}$ ) was collected by the authors in partnership with a dairy farm in Merced, California, which also grows corn and hay – see Table I. We chose a dairy farm for this study due to its economic significance: according to [34], dairy products are the most valuable agricultural commodity in California. The operational data for the small fleet of tractors was obtained using JDLink, a telemetry software provided by the tractor manufacturer (John Deere) and which allowed us to monitor the motor load, daily working hours, among other variables (see Fig. 3). The collected data represents a wide range of farming tasks and loads. For example, tractor  $T_{low}$  consistently operates under low motor loads, with the majority of its tasks demanding less than 20% of the nominal power. In contrast, tractors  $T_{med}$ ,  $T_{high}$ ,  $T_{vhigh}$  are frequently paired with implements that require significantly higher motor loads, ranging between 20% and 80% of the tractor's nominal power.

The amount of working time per day ( $t_{day}$ ) is another crucial element in the mission profile. Fig. 4 represents the cumulative distribution function of  $t_{day}$ , based on the data collected from one year of operation of tractors ( $T_{med}$ ,  $T_{high}$ ,  $T_{vhigh}$ )<sup>1</sup>. Similarly to the motor load, the daily working time also varies from tractor to tractor. For example, tractor  $T_{high}$  is operated for less than 4 hours per day 72% of the time, with an average of 1.5 hours per day. On the other hand, tractor  $T_{vhigh}$  works longer hours, with an average daily working time of 6.8 hours; on rare occasions, it works more than 12 hours per day. Both the motor load and  $t_{day}$  play a significant role in the sizing of the tractor's battery and are critical variables in the TCO analysis. As we will see in later sections, higher motor loads and daily working time require larger onboard energy storage in the tractor, leading to higher costs.

### C. Component Sizing (c)

When acquiring an electric or hybrid tractor, several components need to be sized: i) the nominal power of the tractor ( $P_{nom}$ ); ii) electric motor power ( $P_{nom}^e$ ); iii) the diesel motor power ( $P_{nom}^d$ ); iv) the battery size ( $E_{bat}$ ) and v) the power for recharging the batteries ( $P_{ch}$ ). In this work, we assume that  $P_{nom}$  is defined by the farmer taking into account existing motor-sizing methods, which match the motor power with the needs of the implemented attached to the tractor (see [35]).

<sup>1</sup>The data of  $T_{low}$  was taken from the literature [11] and its daily working time is unknown

TABLE II  
PARAMETERS OF THE TRACTOR MODEL (FOR SIZING PURPOSES)

| Parameter        | Value | Source | Description                        |
|------------------|-------|--------|------------------------------------|
| $\eta_{motor}^*$ | 0.85  | [37]   | avg. motor-inverter efficiency     |
| $\eta_{bat}^*$   | 0.95  | [38]   | battery charging/disch. efficiency |
| $\eta_{ch}^*$    | 0.90  | [39]   | charger efficiency                 |
| $\gamma_{bat}$   | 0.80  | [40]   | battery usable capacity            |
| $t_{ch}^*$       | 12 h  | -      | (overnight) charging time          |
| $V_{bat}^*$      | 400 V | [41]   | battery pack voltage               |

1) *Motor Sizing*: In general, the tractor power is generated by a convex combination of diesel ( $P_{nom}^d$ ) and electric ( $P_{nom}^e$ ) motors:

$$\begin{aligned} P_{nom} &= P_{nom}^e + P_{nom}^d \\ P_{nom}^e &= P_{nom} \gamma_e \\ P_{nom}^d &= P_{nom}(1 - \gamma_e) \end{aligned} \quad (3)$$

where  $\gamma_e \in [0, 1]$  is called the degree of electrification, and  $(P_{nom}^e, P_{nom}^d)$  are the nominal powers of the electric and diesel motors, respectively. In what follows, we will treat  $\gamma_e$  as a design parameter. We will use the TCO model (to be presented shortly) to identify the most suitable  $\gamma_e$  for different types of operations. If  $\gamma_e = 1$ , it means the tractor is fully electric.  $\gamma_e = 0$  renders a full diesel powertrain, and  $\gamma_e \in (0, 1)$  yields a hybrid powertrain.

2) *Battery Sizing*: Let us now look into the sizing of the battery of the electric tractor. The energy storage capability ( $E_{bat}$ ), usually measured in kWh, is a key design decision for the battery. To select  $E_{bat}$ , we assume that the electric tractor is designed to continuously operate with a motor load  $\alpha^*$  and an average daily working time  $t_{day}^*$ . The asterisk denotes a design specification. Assuming a single charge per day, the battery energy needs can be approximated as:

$$E_{bat}(\alpha^*, t_{day}^*) \approx \alpha^* P_{nom}^e t_{day}^* / (\eta_{motor}^* \eta_{ch}^* \gamma_{bat}) \quad (4)$$

where  $\eta_{motor}^*$  is the average driveline efficiency of the electric tractor and accounts for losses in the motor and inverter.  $\eta_{ch}^*$  represents the average charging efficiency, and  $\gamma_{bat}$  is the usable energy in the battery to prevent the high depth of discharge that accelerates battery degradation [36]. Table II contains the values of the parameters employed in this work, which is based on data/assumptions used in recent electric vehicle literature. The hybrid tractor also has a battery that needs to be sized. We assumed that the selection of this battery follows the sizing rule (4). This assumption implies that the hybrid tractor is capable of continuously operate in electric mode during the daily working time  $t_{day}^*$  as long as the load power does not exceed  $P_{nom} \gamma_e \alpha^*$ .

3) *Charger Sizing*: To design  $P_{ch}$ , the tractor battery is assumed to be charged overnight with a charging time  $t_{ch}^*$ . Under this assumption, the charging power is given as:

$$P_{ch}(t_{ch}^*) \approx \gamma_{bat} E_{bat}(\alpha^*, t_{day}^*) / (\eta_{ch}^* t_{ch}^*) \quad (5)$$

where  $\eta_{ch}^*$  is the energy efficiency of the charger.

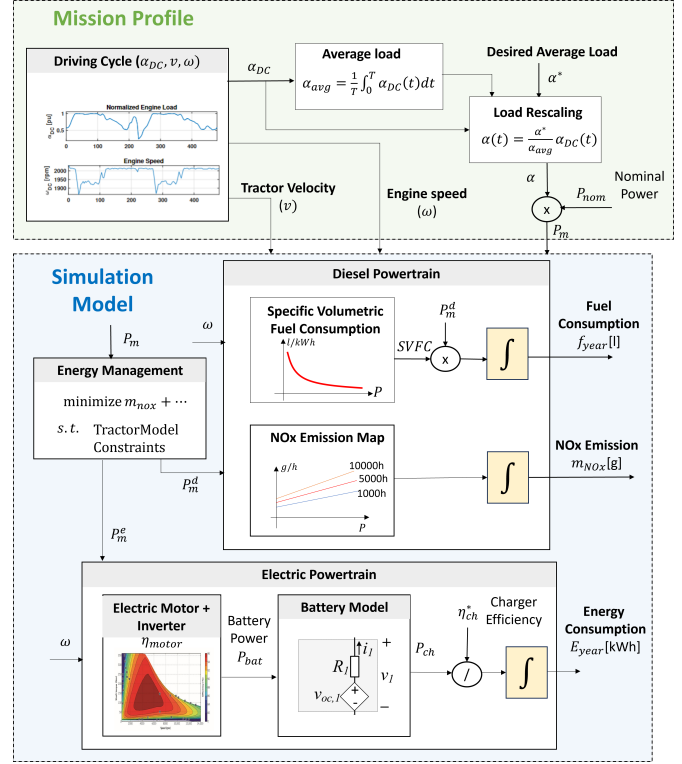


Fig. 5. Overview of the tractor's numerical simulation model.

#### D. Tractor Simulation Model ( $m$ )

This section presents the numerical simulation model employed to estimate tractors' energy consumption and pollutant emissions. As depicted in Fig. 5, we adopt a quasi-static modeling approach, where the powertrain components (battery, electrical motor, diesel engine) are modeled with low-complex models that are easier to implement and parameterize. Since the electric and diesel powertrains are particular cases of the hybrid configuration, this section presents only the simulation model of the hybrid tractor. In this case, the requested tractor power ( $P_m$ ) can be provided by the electric ( $P_m^e$ ) and/or the diesel ( $P_m^d$ ) motors:

$$P_m = P_{nom} \alpha = P_m^e + P_m^d \quad (6)$$

1) *Electric Motor and Battery Model*: To model the energy efficiency of the electric motor and its inverter, we employed an efficiency map  $\eta_{motor}$  dependent on the torque and rotational speed  $\omega$  – see Fig. 6(a). The map is based on a permanent magnet synchronous motor from [37].

The battery pack was modeled using an electrical equivalent circuit composed of an open-circuit voltage ( $OCV(q)$ ) and an equivalent series resistance ( $R_s(q)$ ), both dependent on the state of the charge ( $q$ ) [42]:

$$\dot{q} = -\frac{1}{C_{bat}} i_{bat} \quad (7)$$

where  $C_{bat}$  is the nominal battery pack capacity (in [A.s]) and  $i_{bat}$  is the current. The current requested by the battery is obtained by solving the following power balance equation:

$$P_{bat} = \frac{P_m^e}{\eta_{motor}} = (OCV(q) - R_s(q)i_{bat})i_{bat} \quad (8)$$

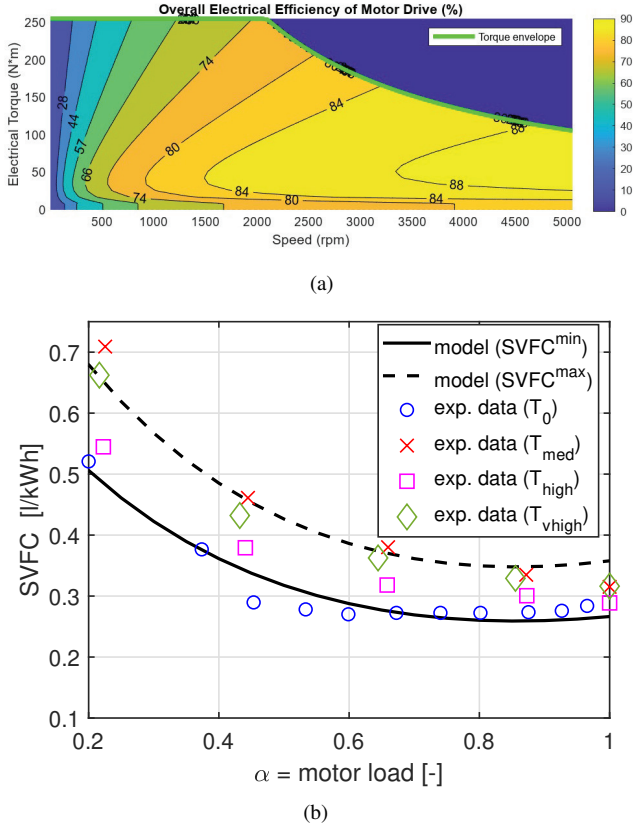


Fig. 6. a) efficiency map of the electrical motor; b) Specific volumetric fuel consumption (SVFC) of the diesel engine with parameterization  $SVFC^{\min}$  (full line) and  $SVFC^{\max}$  (dashed line) vs experimental data for tractors  $T_0, T_{med}, T_{high}, T_{vhight}$ .

where  $P_{bat}$  is the power that the electric drive requests from the battery considering the overall efficiency of the motor drive ( $\eta_{motor}$ ). The battery pack comprises  $n_s$  cells in series and  $n_p$  parallel. We selected  $n_s$  based on the nominal voltage  $V_{bat}^*$  of the battery pack, while  $n_p$  was based on energy requirements:

$$n_s = V_{bat}/OCV_n \quad (9)$$

$$n_p = E_{bat}/(n_s V_{bat}^* C_{bat,cell}) \quad (10)$$

where  $OCV_n$  corresponds to the nominal voltage of each individual cells and  $C_{bat,cell}$  the cell capacity<sup>2</sup>.

The battery parameters were calibrated to match the data sheets of the cells provided by the battery manufacturer's (A123: AMP20M1HD) [43].

2) *Diesel Engine*: Diesel engines have significant energy losses when converting fuel energy into mechanical power. Heating, pumping, and friction losses are some of the main factors that reduce the energy efficiency of these engines [33]. To account for these losses, we use the specific volumetric fuel consumption (SVFC) map of the engine, which provides a normalized indicator of the fuel consumption rate with respect to the amount of work being done by the engine:

$$\dot{f}_{fuel} = SVFC(\alpha) P_m^d \quad (11)$$

<sup>2</sup>Note that  $C_{bat} = n_p C_{bat,cell}$

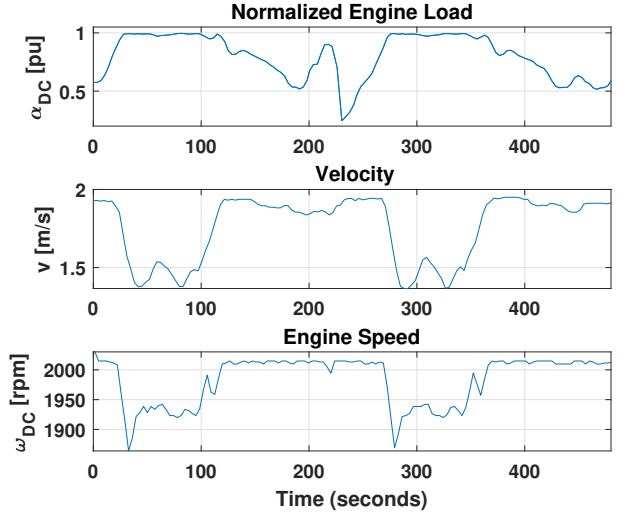


Fig. 7. Example of a time-domain mission profile for the tractor (DLG - Mixed Cycle).

where  $\dot{f}_{fuel}$  [l/h] is the fuel rate and  $P_m^d$  the power developed by the diesel engine. The mathematical model of the SVFC [l/kWh] is based on the parameterization proposed in the standard ASAE D497.4 [44]:

$$SVFC(\alpha(t)) = \theta_{d1} + \theta_{d2}\alpha(t) - \theta_{d3}\sqrt{\theta_{d4}\alpha(t) + \theta_{d5}} \quad (12)$$

where  $\theta_{di}$ ,  $i \in \{1, 2, 3, 4, 5\}$  are parameters.

Fig. 6(b) shows the SVFC for the tractors  $T_{med}, T_{high}, T_{vhight}$ , as obtained from the Nebraska Tractor Test Lab [45]. Since data for tractor  $T_{low}$  is unavailable<sup>3</sup>, we substituted it with the SVFC of tractor  $T_0$  (*Fendt 211 S Vario*), whose test data is publicly available from the German Agricultural Society (DLG) [46] and serves as an alternative option with high fuel efficiency. Inspecting Fig. 6(b) reveals that the fuel consumption trend is consistent across all tractors: as engine load increases, more efficient operating regions are achieved, resulting in lower fuel consumption. For example, the SVFC at high engine load ( $\alpha = 0.8$ ) is nearly half the SVFC observed at low loads ( $\alpha = 0.2$ ). The figure also displays the fitting of two SVFC models: the first, denoted  $SVFC^{\min}$ , is calibrated to fit  $T_0$  (the tractor with the lowest fuel consumption), while the second,  $SVFC^{\max}$ , is fitted to  $T_{med}$  (the tractor with the highest fuel consumption).

Note that since SVFC is a normalized variable, the model (11) can be used to estimate the fuel consumption of tractors with different engine powers. The underlying assumption is that SVFC remains constant as the engine size scales [47]. In the following analysis, we consider an "optimistic" fuel efficiency scenario and use  $SVFC^{\min}$  in most of the numerical simulations. This reflects the expectation that future diesel tractors will continue improve fuel efficiency. The "pessimistic" scenario  $SVFC^{\max}$  is tackled via sensitivity analysis.

3) *Re-scaling of (power) load*: The experimental data collected by the authors (presented in Section II-B) has a very

<sup>3</sup>The data for  $T_{low}$  was obtained from the literature [11], and the specific engine details are not known.

low sampling rate (1 hour) and does not provide enough information to represent the tractor's mission accurately. To overcome this limitation, we decompose the operating cycle of the tractor into two phases. The first phase focuses on a fast time scale and provides a second-by-second profile for the engine load  $\alpha_{DC}(t)$ , velocity  $v_{DC}(t)$  and engine speed  $\omega_{DC}(t)$ . This work employs the DLG's mixed cycle profile [48], depicted in Fig. 7. The second phase tackles the slow time scales; it re-scales the average engine load to capture different working intensities associated with different farming tasks. This re-scaling is performed by changing the average value of the tractor load:

$$\alpha(\alpha^*, \alpha_{DC}(t)) = \frac{\alpha^*}{\frac{1}{T} \int_0^T \alpha_{DC}(t) dt} \alpha_{DC}(t) \quad (13)$$

where  $T$  is the duration of the normalized mission profile, and  $\alpha^*$  is a parameter that allows us to change the average load of the tractor. This parameter may be changed, for example, from hour to hour or by day to day.

Note that in our tractor model, the rotational speed  $\omega$  is treated as an exogenous signal that is provided by the mission profile<sup>4</sup>. This approach reduces model complexity, since it avoids using the (inverse) gearbox model – and its complicated gearshift patterns – to compute  $\omega$  based on the linear tractor velocity. This also helps us accelerate the tractor's simulation model, which is particularly useful in the sensitivity analysis presented in Section IV, where a large number operating conditions need to evaluated via simulation.

4) *Energy/Fuel Consumption and Emissions*: The yearly fuel usage of the tractor is computed by time integration of the fuel rate, while the electrical energy relies on the integration of the power provided by the battery:

$$f_{year}(\alpha(t), T_{year}) = \int_0^{T_{year}} SVFC(\alpha(t)) P_m^d(t) dt \quad (14)$$

$$E_{year}(\alpha(t), T_{year}) = \int_0^{T_{year}} \frac{P_{bat}(t) + R_s(q(t)) i_{bat}(t)^2}{\eta_{ch}^*} dt$$

where  $f_{year}$  is the fuel consumption per year,  $T_{year}$  is the total number of working hours per year of the tractor, and  $P_m^d(t)$  is the instantaneous motor power. The energy consumption  $E_{year}$  also takes into account Joule losses in the battery ( $R_s i_{bat}^2$ ) and losses in the charger's power converter ( $\eta_{ch}^*$ ).

To model the NOx emissions of the engine, we adopt the framework proposed by CARB [49], which assumes that the time rate of NOx generation is proportional to the power consumption of the engine:

$$m_{NOx} = \int_0^{T_{year}} P_m^d(t) EF dt \quad (15)$$

$$EF = (EF_0 + EF_{DR} t) FCF \quad (16)$$

where  $m_{NOx}$  is the amount of NOx generated by the engine (in [g]), and  $EF$  is a normalized emission factor (in [g/hp.h]), which grows linearly with the amount of time that the engine is used ( $t$ ). This model has three parameters: i)  $EF_0$

<sup>4</sup>Note that in our powertrain configuration, the diesel engine and electric motor are installed in the same shaft (see Fig. 2). This means that they have the same rotation speed  $\omega$ .

TABLE III  
MPC PARAMETERS

| Parameter        | Value           | Description          |
|------------------|-----------------|----------------------|
| $T_s$            | 1               | Sample Time          |
| $N$              | 300             | Prediction Horizon   |
| $\Delta q^{max}$ | 0.02            | Final SoC tolerance  |
| $\rho$           | 0.0004          | Trade-off parameter  |
| $q^{max}$        | 0.98            | max. SoC             |
| $q^{min}$        | 0.2             | min. SoC             |
| $i_{bat}^{max}$  | $3C_{bat}$      | maximum bat. current |
| $i_{bat}^{min}$  | $i_{bat}^{max}$ | minimum bat. current |

is the zero-hour emission factor (in [g/hp.h]); ii)  $EF_{DR}$  is the deterioration rate that captures the increase in emissions as the engine ages (in [g/hp.h<sup>2</sup>]); and iii)  $FCF$  is a fuel correction factor (unit-less) [49]. The first two parameters are further dependent on the engine's nominal horsepower and production year. The value of these parameters were calibrated to represent the average emissions off-road diesel tractors in operation in California [50] (see Fig. 22 in Appendix A).

5) *Energy Management*: A model predictive control (MPC) framework [26] was employed to manage the hybrid powertrain's energy and decide on how to split the power between the electric and diesel motors. To improve the environmental benefits of hybrid tractors, our MPC aims to minimize NOx emissions while considering a prediction model of the battery and operational constraints, such as power and SoC limits. The critical elements of the prediction model include the battery SoC dynamics (7) and power balance constraints between energy storage and load. Initially formulated in continuous time, this model was discretized with the Euler method and a sample time  $T_s = 1$ s. The resulting MPC optimization problem is formulated as follows:

$$\min \quad (1 - \rho) \hat{m}_{NOx}(P_m^d[k]) + \rho \left( \frac{q[N] - q^*[N]}{\Delta q^{max}} \right)^2$$

s.t.

$$q[k+1] = q[k] - \frac{T_s}{C_{bat}} i_{bat}[k], \quad (17)$$

$$q[0] = q_0 \quad (18)$$

$$\frac{P_m^e[k]}{\eta_{motor}[k]} = (OCV(q[k]) - R_s(q[k]) i_{bat}[k]) i_{bat}[k]$$

$$\alpha[k] P_{nom} = P_m^e[k] + P_m^d[k] \quad (19)$$

$$\alpha[k] = \hat{\alpha} \quad (20)$$

$$q^*[k] = q[0] - m T_s k \quad (21)$$

$$q^{min} \leq q[k] \leq q^{max} \quad (22)$$

$$0 \leq P_m^d[k] \leq P_{nom}^d \quad (23)$$

$$i_{bat}^{min} \leq i_{bat}[k] \leq i_{bat}^{max} \quad (24)$$

$$k = 0, \dots, N - 1 \quad (25)$$

where  $k$  represents the discrete time index, and  $N$  is the number of samples used in the prediction horizon.

The MPC cost is composed of two terms. The first term,  $\hat{m}_{NOx}$ , captures the *normalized* NOx emissions during the

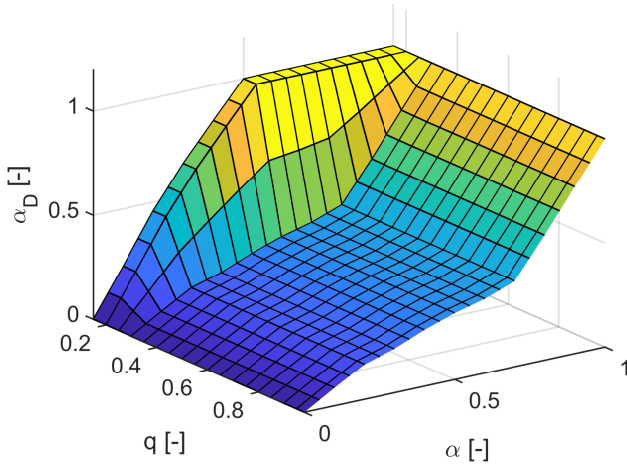


Fig. 8. MPC lookup table for calculation of the optimal diesel engine power based on battery SoC  $q$  and tractor load  $\alpha$  (note: the vertical axis denotes the normalized diesel power:  $\alpha_D = P_m^d / P_{nom}^d$ ; lookup table generated for  $\gamma_e = 0.5$ .)

prediction horizon. It is computed via the discretization of (15):

$$\hat{m}_{NOx}(P_m^d[k]) = \sum_{i=0}^{N-1} \frac{1}{m_{NOx}^{max}} (EF \cdot P_m^d[k] \cdot T_s) \quad (26)$$

where  $m_{NOx}^{max}$  is the amount of NOx that the diesel engine would generate if it were operating at maximum power ( $m_{NOx}^{max} = EF \cdot P_{nom}^d \cdot T_s$ ). The second cost term penalizes quadratic differences between the final SoC ( $q[N]$ ) and the reference SoC ( $q^*[N]$ ). It prevents the accelerated discharge of the battery (note that  $P_m^d = 0$  would minimize the NOx emissions during the prediction horizon but would quickly discharge the battery). The parameter  $\Delta q^{max}$  represents an expected "tolerance" for SoC deviation at the end of the prediction horizon. The parameter  $\rho$  is a trade-off weight that allows the designer to balance the two normalized costs. In this work, we used a time-dependent model for the reference battery SoC, which decreases linearly with the usage time of the tractor:

$$q^*[k] = q[0] - mT_s k \quad (27)$$

$$m = \frac{q^{max} - q^{min}}{t_{day}} \quad (28)$$

where  $m$  is the time rate of SoC decrease  $[-/s]$ .

The MPC constraints are composed of the i) discretized battery SoC dynamics (17) and initial SoC condition (18); ii) power balance between battery, electric and diesel motors (19); iii) preview model for the tractor load ( $\alpha$ ) and reference SoC for the battery ( $q^*$ ), (20)-(21); and iv) SoC, power and current limits(22)-(24). The preview model assumes that the engine load remains constant during the prediction horizon:  $\alpha[k] = \hat{\alpha}$ , where  $\hat{\alpha}$  is the expected load during the prediction horizon. In this work we computed  $\hat{\alpha}$  based on the current load ( $\hat{\alpha} = \alpha[0]$ ). This assumption is reasonable because tractors often operate for long periods with constant velocity/load. The power balance constraint depends on the motor efficiency

$\eta_{motor}[k]$ , which varies with rotational speed and torque and is nonlinear. To simplify the MPC prediction model, we assumed an average motor efficiency  $\eta_{motor}[k] = \eta_{motor}^*$ . Table III summarizes the values of the MPC parameters employed in this work.

The implementation of the MPC is performed in a receding-horizon framework: at each time step, the initial conditions ( $q_0, \hat{\alpha}$ ) are updated, the MPC optimization problem is solved, and the resulting optimal power split ( $P_m^d, P_m^e$ ) applied to the tractor. Note that the MPC problem depends on two initial parameters ( $q_0, \hat{\alpha}$ ). To accelerate the calculation of the MPC's optimal solution, we i) computed "offline" the optimal power split<sup>5</sup> for a grid of values for the initial conditions ( $q_0, \hat{\alpha}$ ); ii) stored this information in a lookup table and finally iii) employed linear interpolation to determine the optimal solution "online." Fig. 8 provides an example of the MPC lookup table generated by this approach.

### III. ECONOMIC MODEL

The TCO is computed as a summation of multiple cost factors:

$$TCO^j = C_{veh}^j + C_{infra}^j + C_{energy}^j + C_{other}^j \quad (29)$$

where the superindex  $j \in \{d, e, h\}$  denotes the type of drivetrain ( $d =$ diesel,  $e =$ electric,  $h =$ hybrid) and

- $C_{veh}$  is the tractor acquisition cost, which includes all the costs related to the purchase of the tractor, taxes, and financing.
- $C_{infra}$  is the infrastructure cost for acquiring the battery charger and upgrades to the electrical infrastructure of the farm.
- $C_{energy}$  represents the energy costs due to fuel consumption in the diesel driveline and electricity costs to recharge the tractor battery in the electric driveline.
- $C_{other}$ : the additional costs include housing, insurance, lubricants, maintenance and repairs (M&R), and mid-life costs.

#### A. Vehicle Costs

The vehicle costs include all the acquisition costs associated with the tractor purchase, taxes, and financing. To facilitate the computation of this cost, the tractor components are divided into two cost groups: i) energy storage and power conversion and ii) glider. The former group accounts for the battery pack ( $c_{bat}$  [\$/kWh]), electric motor & inverter ( $c_{emotor}$  [\$/kW]) and diesel engine ( $c_{dmotor}$  [\$/kW]) costs. The latter ( $c_{glider}$  [\$/kW]) takes into account the cost of the remaining components, such as chassis, wheels, mechanical transmission, etc. Apart from the battery, all the other costs are normalized with respect to nominal motor power. The overall purchase price of the tractor is defined as:

$$\begin{aligned} C_{veh}^j = & (1 + c_{tax})(c_{dmotor}^j p_{nom} + c_{emotor}^j p_{nom} \\ & + c_{bat}^j E_{bat} + c_{glider}^j p_{nom}) + c_{finance}^j \end{aligned} \quad (30)$$

<sup>5</sup>this solution was obtained via an interior point optimizer [51];

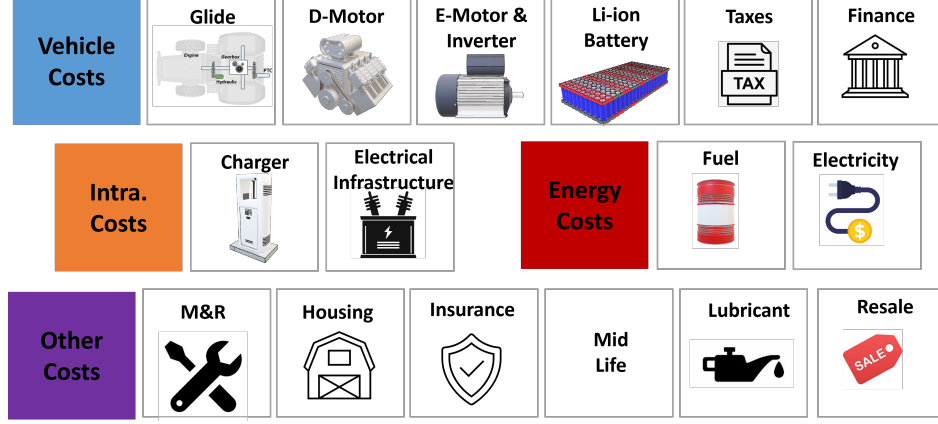


Fig. 9. Overview of the vehicle, infrastructure, energy, and other costs employed in calculating the economic analysis of tractors.

This price takes into account sales taxes  $c_{tax}$ , (assumed to be 8.5%) and also the financing costs  $c_{finance}^j$  that the farmer needs to pay to raise funds for the purchase (5 year loan at 3% interest rate). Depending on the powertrain type, some component costs will be zero, e.g., a diesel tractor does not require a battery or electric motor, hence  $c_{bat}^d = 0$  and  $c_{motor}^d = 0$ .

The value of the above parameters was determined based on previous TCO studies of electric vehicles; their values are summarized in Table IV. The glider cost is one of the most difficult parameters to obtain since manufacturers usually do not disclose the individual cost breakdown of tractors. Previous studies have suggested that the diesel motor represents 20% of the overall costs of the tractor [11], [33]; as a result, we assume that the glider cost is linearly proportional to the cost of the diesel engine:  $c_{glider}^j = \frac{1}{0.2}c_{motor}^d$ . The cost of the battery pack is another critical factor in the TCO model. Electric tractors have a lower production volume than on-road vehicles, so the battery manufacturing and assembly costs are expected to be higher. To capture this issue, we adopt the approach suggested in [52] and parameterize  $c_{bat}^j$  using automotive battery prices [53] with a 5-year delay.

### B. Infrastructure Costs

The infrastructure costs account for the acquisition of i) the off-board battery charger and ii) upgrades to the farm's infrastructure to support the higher electricity demand. The latter cost might be particularly relevant in farms located in remote areas, with poor connection to the electric grid which might need extra upgrades to the transformer, cabling, conduits, etc [58] [59]. The overall infrastructure costs are modeled as follows:

$$C_{infra}^j(P_{ch}) = c_{ch}^j(P_{ch})P_{ch} + c_{infra,upg}^j(P_{ch})P_{ch} \quad (31)$$

where  $c_{ch}^j$  [\$/kW] is the charger cost, and  $c_{infra,upg}^j$  [\$/kW] is the normalized cost to upgrade the electrical infrastructure. Both costs depend on the charging power  $P_{ch}$ . The tractor's batteries can be charged with Level 1, Level 2, and DC fast charging [58]. Level 1 is a low-power charging mode ( $\approx 1.4$  kW), which requires a traditional 120Vac electric installation.

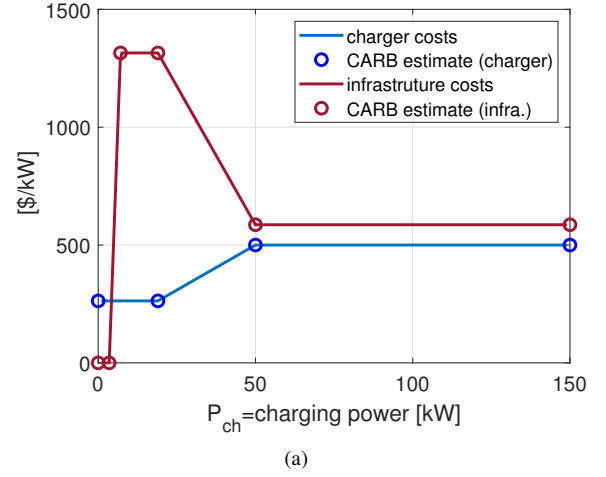


Fig. 10. Piece-wise linear model for charger ( $c_{ch}$ ) and electrical infrastructure costs ( $c_{infra,upg}$ ). The plots also show the cost estimate from CARB [52], which was used to derive the piece-wise linear model.

Level 2 and DC fast charging ( $\geq 50$ kW) offer significantly higher charging power but require higher voltage levels and farm infrastructure upgrades. Fig. 10 depicts the model for  $c_{ch}$  used in this work. It relies on the linear interpolation of the CARB's charger cost estimates developed for medium- and heavy-duty on-road electric vehicles [52], which share similar charging needs as electric tractors. This model produces a normalized charging cost  $c_{ch}^j(P_{ch})$  that increases linearly at low charging power and then saturates once power reaches 50 kW.

Fig. 10 also shows the normalized infrastructure cost  $c_{infra,upg}^j$ . We assume that the existing farm's electrical infrastructure can support low-power (Level 1) charging without extra cost. We developed a piece-wise linear model for a higher charging power that interpolates the cost estimate provided by [52]. This model assumes an upgrade cost of 1315 \$/kW for Level 2 charging, which then drops to 586 \$/kW as we approach fast DC charging. As discussed in [58], infrastructure costs do not rise proportionally with charging power. Several costs need to be considered when upgrading the electrical infrastructure, including labor, materials, and permits. For ex-

TABLE IV  
SUMMARY OF THE PARAMETERS EMPLOYED IN THE ECONOMIC MODEL

| Parameter                     | Value                             | Source     | Description  |
|-------------------------------|-----------------------------------|------------|--|
| $c_{dmotor}^d$                | 128 \$/kW                         | [54]       | normalized cost of the diesel motor                    |
| $c_{emotor}^e$                | 40 \$/kW                          | [11]       | normalized cost of the electric motor and inverter     |
| $c_{bat}^e$                   | 200 \$/kWh                        | [53]       | normalized cost of the battery                         |
| $c_{glider}^j$                | $5c_{dmotor}^d$                   | [11], [33] | normalized glider costs                                |
| $c_{tax}$                     | 8.5%                              | [55]       | sales taxes (based in California)                      |
| $c_{finance}^j$               | -                                 | -          | financing costs (5 years with 3% interest rate )       |
| $C_0^j$                       | $C_{veh}^j - C_{finance}^j$       | -          | purchase price (without financing costs)               |
| $C_{house}^j$                 | $n_{life} \frac{0.2}{100} C_0^j$  | [20]       | housing costs  |
| $C_{insurance}^j$             | $n_{life} \frac{0.25}{100} C_0^j$ | [20]       | insurance costs  |
| $k_{lub}$                     | 0.1                               | [20]       | fraction of lubricant cost (w.r.t. fuel cost)          |
| $k_1$                         | 0.0069                            | [44]       | parameter of the M&R cost model                        |
| $k_2$                         | 2                                 | [44]       | parameter of the M&R cost model                        |
| $k_e$                         | 0.625                             | [52], [56] | fraction of electric M&R costs (w.r.t. diesel tractor) |
| $n_{cycles}$                  | 1500                              | [57]       | number of charge/discharge cycles                      |
| $k_{midlife}$                 | 0.5                               | [57]       | cost reduction of the battery at time of replacement   |
| $(C_{rs1}, C_{rs2}, C_{rs3})$ | (0.981, 0.093, 0.0058)            | [20]       | parameters of resale value model                       |

ample, installing a 25 kW and a 50 kW charging system might require the same amount of labor but different materials costs, contributing to a reduction in the normalized infrastructure upgrades costs [\$/kW]—especially in cases where labor is the dominant cost factor. It is important to note that the expenses in infrastructure upgrades will vary from farm to farm and are highly dependent on their existing connection to the grid (e.g., farms far away from electrical power sources might incur significant trenching costs [60]).

Note: we assume that diesel tractors do not require modifications to the existing refueling infrastructure of the farm ( $C_{infra}^d = 0$ ).

### C. Energy Costs

The energy costs are due to fuel consumption in the diesel driveline ( $C_{energy}^d$ ) and electricity costs ( $C_{energy}^e$ ) to recharge the tractor battery in the electric driveline. In the diesel driveline, the total fuel costs are computed as follows:

$$C_{energy}^d = \sum_{k=1}^{n_{life}} c_{fuel,k} f_{year} \quad (32)$$

where  $c_{fuel,k}$  is the fuel cost [\$/l] in year  $k$ ,  $n_{life}$  the expected lifetime of the tractor (in years),  $f_{diesel}$  is the fuel consumption of the tractor per year. This work assumes that the tractor is subject to the same mission profile (and fuel consumption) every year. The short-term fuel cost prediction ( $k \in [0, 10]$ ) is based on the California Energy Commission's fuel forecast [52], adjusted to today's dollars using the California consumer price index – see Fig. 11. Long-term fuel cost predictions ( $k > 10$ ) employ the annual percentage change in the U.S. Energy Information Administration (EIA) prices [61].

In the electric tractor case, the energy costs  $C_{energy}^e$  are computed analogously, using electricity consumption instead of fuel:

$$C_{energy}^e = \sum_{k=1}^{n_{life}} c_{ele,k} E_{year} \quad (33)$$

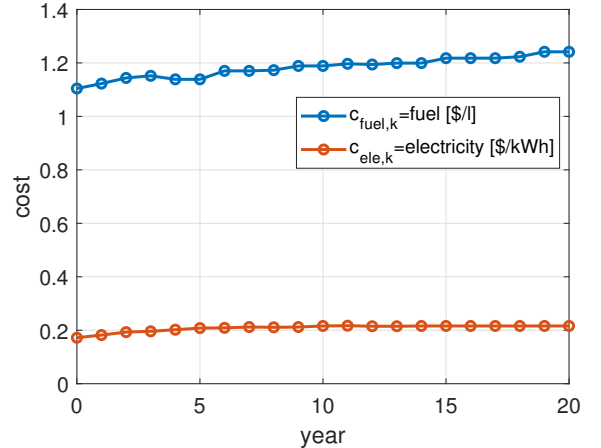


Fig. 11. Normalized fuel and electricity cost forecast

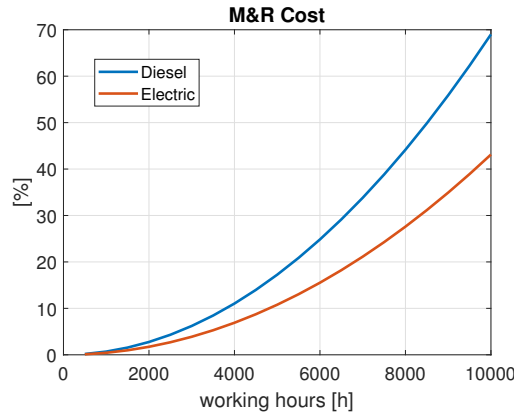


Fig. 12. Maintenance and repair (M&R) cost model, normalized with respect to purchase price ( $C_0$ ).

where  $c_{ele,k}$  is the electricity cost [\$/kWh] in the year  $k$  and  $E_{year}$  the energy needed to re-charge the tractor. The energy consumption  $E_{year}$  considers the energy efficiency of the motor, battery, and charger, as discussed in Section II-C.

The electricity cost  $c_{ele,k}$  was based on the California Energy Commission's forecast [52] and adjusted to today's dollars using California consumer price index. It is depicted in Fig. 11.

#### D. Other Costs

The other tractor costs ( $C_{other}^j$ ) include housing, insurance, lubricants, maintenance and repairs (M&R), mid-life and resale costs:

$$\begin{aligned} C_{other}^j &= C_{house}^j + C_{insurance}^j + c_{lub}^j + \\ &C_{M\&R}^j + C_{midlife}^j + C_{resale}^j \end{aligned} \quad (34)$$

The housing is important to protect the tractor during periods of inactivity; this is particularly critical in electric tractors with temperature-sensitive components (e.g., battery) that need to be stored in areas where temperatures are not too cold or hot. We assume that the yearly housing costs ( $C_{house}^j$ ) represent 0.2% of the purchase price, while the insurance costs ( $C_{insurance}^j$ ) accounts for 0.25% [20].

The lubricant costs in the diesel powertrains are assumed to be linearly proportional to the fuel cost:  $c_{lub}^j = k_{lub} C_{energy}^j$ . The M&R considers routine replacement of worn parts and repair of accidental damage. According to the standard ASAE496.2 [22], the average M&R costs of a diesel tractor follows an exponential curve:

$$C_{M\&R}^d(T_{year}) = C_0^d k_1 \left( \frac{n_{life} T_{year}}{1000} \right)^{k_2} \quad (35)$$

where  $k_1$  and  $k_2$  are parameters and  $C_0^d = C_{veh}^d - c_{finance}^d$  the purchase price (without financing). Electric drivelines usually have more affordable M&R costs because of the lower number of moving parts in electric motors. In this work, we assume that the M&R costs of the electric tractor are linearly proportional to their diesel counterpart:

$$C_{M\&R}^e = k_e C_{M\&R}^d \quad (36)$$

where  $k_e$  is a constant of proportionality. Reference [52] indicated that electric drivelines can offer up to 50% lower M&R costs than diesel, while [56] estimates cost reduction of 25%. Our work assumes an intermediate value between these two estimates ( $k_e = 0.625 = \frac{0.75+0.5}{2}$ ).

Another critical cost component in the electric tractor is the replacement of the battery during the tractor's lifetime. Battery ages with time and charge/discharge cycling, reducing the amount of power and usable energy. Usually, the battery manufacturer provides a maximum number of charge-discharge cycles  $n_{cycles}^*$  that the battery can withstand before reaching its end-of-life condition (usually 80% of their rated capacity). Analysis performed by [57] indicates that  $n_{cycles}^*$  usually varies between 1000 and 3000 cycles in road electric vehicles. If this number of cycles is exceeded, the battery must be replaced. We model this replacement cost using the following approximation:

$$C_{midlife}^e = \begin{cases} 0 & n_{cycles} < n_{cycles}^* \\ k_{midlife} C_{bat}^j E_{bat} & \text{otherwise} \end{cases} \quad (37)$$

where  $k_{midlife}$  is a ratio that captures a future cost decrease in the battery at the time of the replacement and  $n_{cycles}$

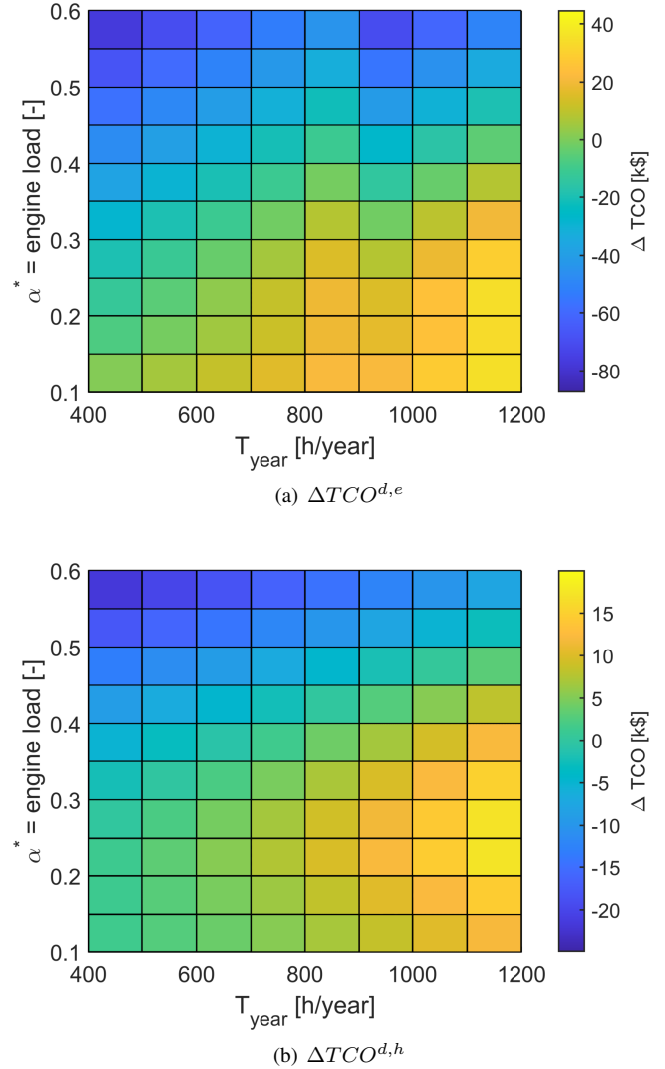


Fig. 13. TCO difference between a) electric and diesel and ( $\Delta TCO^{d,e}$ ) b) hybrid powertrain and diesel ( $\Delta TCO^{d,h}$  ).

is the number of charge-discharge cycles that the battery experienced. Assuming a single charge per working day, we have  $n_{cycles} \approx n_{life} T_{year} / t_{day}$ . In this work, we consider  $k_{midlife} = 0.5$ ; this aligns with the forecasts discussed in [57], which indicates that the battery price should decrease by up to 50% over the next ten years.

The resale cost, also known as salvage value, represents the expected revenue the farmer might obtain by selling the tractor at the end of its useful life. It is modeled here as [20]

$$C_{resale}^j = -C_0^j (C_{rs,1} - C_{rs,2} \sqrt{n_{life}} - C_{rs,3} \sqrt{T_{year}})^2 \quad (38)$$

where  $C_{rs,1}, C_{rs,2}$  and  $C_{rs,3}$  are parameters. It is worth noticing that this cost is negative because it represents revenue.

## IV. RESULTS AND DISCUSSION

This section presents the techno-economic analysis of the electric and hybrid tractor and its comparison against a baseline scenario (diesel powertrain).

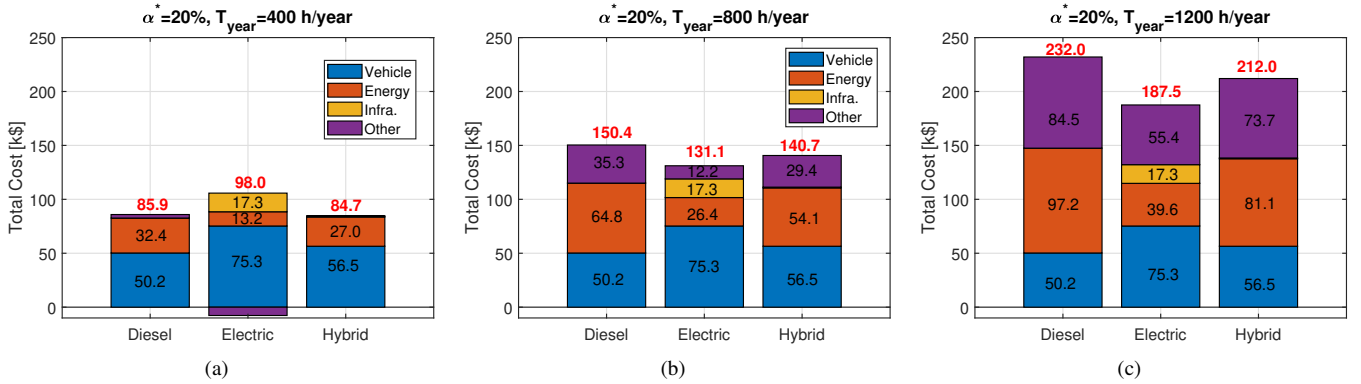


Fig. 14. Cost breakdown of total cost of ownership (TCO) for diesel and electric.

#### A. Impact of engine load and annual working time

First, we investigate the TCO impact of two key parameters: i) average engine load  $\alpha^*$  and ii) total number of working hours per year  $T_{year}$ . To facilitate the comparison between these tractors, we introduce the difference in TCO between diesel and electric powertrains:

$$\Delta TCO^{d,e}(\alpha^*, T_{year}) = TCO^d(\alpha^*, T_{year}) - TCO^e(\alpha^*, T_{year})$$

Positive  $\Delta TCO^{d,e}$  means that the electric option is more affordable than diesel over the tractor's lifetime, while negative  $\Delta TCO^{d,e}$  implies cost benefits for the diesel driveline. In this study, we consider a nominal motor power  $P_{nom} = 70\text{hp}$ , daily operation time  $t_{day}^* = 8\text{h/day}$ , and lifetime  $n_{year} = 15\text{ years}$ . An "optimistic" fuel consumption map for the diesel engine  $SVFC^{min}$  is also initially assumed.

Fig. 13(a) depicts the  $\Delta TCO^{d,e}(\alpha^*, T_{year})$ . The results reveal two main trends: i) as the annual working time  $T_{year}$  increases, the cost difference  $\Delta TCO^{d,e}$  raises, and the economics become more attractive for electric tractors; ii) similarly, lighter loads  $\alpha^*$  also favor electric powertrains. To understand the reason behind this trend, performing a cost breakdown of the tractor is useful. Fig. 14a shows this breakdown for an average load  $\alpha^* = 0.2$  and  $T_{year}=400\text{h/year}$ . In this case, the initial acquisition cost of the electric tractor (\$75k) represents a significant portion of the overall costs of ownership ( 76%); we can also observe that the (electrical) energy costs are significantly lower than the diesel fuel costs (\$13k vs. \$32k). Still, they are not enough to offset the electric tractor's high initial acquisition and infrastructure costs. The TCO of the electric tractor is \$13k more expensive than the diesel counterpart, corresponding to a cost increase of 32%.

Fig. 14(c) shows the cost breakdown for a second use case with high yearly usage,  $T_{year}=1200\text{h/year}$  and average load  $\alpha^* = 20\%$ . In this case, the fuel cost of the diesel tractor (\$97k) represents the dominant factor in the TCO, capturing almost 41% of the total costs of ownership (\$232k). On the other hand, the electric tractor reveals more attractive economics: the energy costs are reduced to \$39.6k, and the total charges are lowered to \$187k, representing 19% of cost savings in comparison to diesel powertrains.

#### B. Impact of working time/day

Next, we focus on identifying operating conditions ( $p = (\alpha^*, T_{year})$ ), under which electric tractors are more affordable than diesel. Mathematically, this means computing the set

$$P^* = \{p : \Delta TCO^{d,e}(p) > 0\} \quad (39)$$

We then perform sensitivity analysis to understand the impact of different parameters (working time per day, battery cost, and tractor's lifetime) in the size of  $P^*$ .

We start by considering the impact of working time per day in  $P^*$ . Fig. 15a shows  $P^*$  for 4h and 8h working day. For  $t_{day} = 4\text{h}$ , the electric tractors are economically competitive for loads as high as 0.6 and  $T_{year} > 1000\text{h/year}$ . However, reducing the daily work time might not be suitable for all farms. For example, in the data collected on the Merced farm (see Fig. 4), one of the tractor ( $T_{vhigh}$ ) had an average usage time of 7 hours per day.

#### C. Impact of battery cost

Let us analyze the impact of the battery cost in  $P^*$ . With increased mass production of electric vehicles, the cost of battery packs (\$/kWh) has been steadily decreasing over the last decade [62]; it is expected that this downward trend will continue in the next years [63]. Fig. 15b shows that, as the battery cost decreases, the electric tractor becomes economically attractive in a wide range of operations. Our study reveals that the electric tractor achieves cost parity with diesel tractor when the battery cost reach 50 – 100\$/kWh for the average operating conditions of tractors in California ( $\alpha^* \approx 0.48$  and  $T_{year} = 800\text{h/year}$  [64]), which is highlighted with a star in Fig. 15.

#### D. Impact of Fuel Price and Efficiency

Another key factor influencing the overall TCO of diesel tractors is fuel price, which is both highly uncertain and volatile. To better understand its impact, we consider three scenarios for the future evolution of fuel prices:

- Scenario A: Baseline fuel price  $c_{fuel,k} = c_{fuel,k}^*$ , where  $k$  is the year and  $c_{fuel,k}^*$  is the nominal predicted fuel cost as shown in Fig. 11.

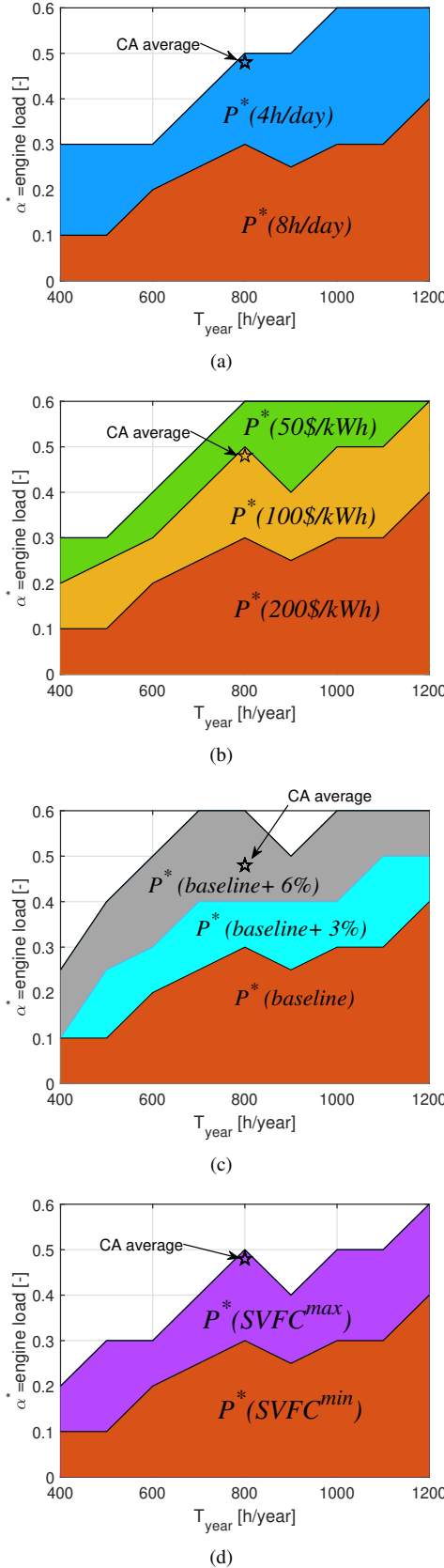


Fig. 15. Sensitivity analysis of the set  $P^*$  for different a) working time per day; b) battery costs; c) annual increase in fuel price d) fuel efficiency maps. The star mark depicts the average operating conditions of tractors in California ( $\alpha = 0.46$  and  $T_{year} = 800\text{h/year}$ ).

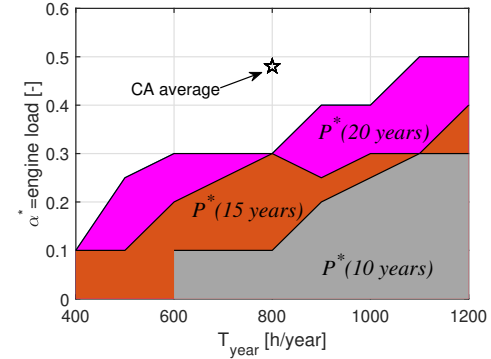


Fig. 16. Sensitivity analysis of the set  $P^*$  for different tractor's lifetime. The star mark depicts the average operating conditions of tractors in California ( $\alpha = 0.46$  and  $T_{year} = 800\text{h/year}$ ).

- Scenario B: Baseline case with an additional 3% annual price increase ( $c_{fuel,k} = c_{fuel,k}^*(1 + 0.03)^k$ ).
- Scenario C: Baseline case with an additional 6% annual price increase ( $c_{fuel,k} = c_{fuel,k}^*(1 + 0.06)^k$ ).

Fig. 15c illustrates  $P^*$  under these scenarios. As expected, higher fuel costs expand the operating conditions under which electric tractors become more cost-effective than diesel powertrains. Under Scenario C, electric tractors would be more affordable than diesel for the average operating conditions in California. A similar outcome is also obtained when diesel engines with high fuel consumption ( $SVFC^{max}$ ) is used in the numerical simulation - see Fig. 15d.

#### E. Impact of Lifetime

Fig. 16 depicts the impact of the tractor's lifetime in  $P^*$ . It can be observed that as the tractor's lifetime increases, the electric tractor becomes more attractive, offering lower costs in a wider operating range. This can be explained by the additional savings with energy costs accumulated over the electric tractor's lifetime, offsetting their more considerable acquisition costs, as well as battery replacement costs (as discussed in Section III-D).

#### F. Hybrid Powertrain

Next, we focus on the TCO of hybrid powertrains. We first investigate the selection of optimal electrification ratio  $\gamma_e^*$  that minimizes the TCO for the different average engine loads ( $\alpha^*$ ) and operating time per year ( $T_{year}$ ). This ratio can be determined by solving the following optimal sizing problem:

$$\gamma_e^*(\alpha^*, T_{year}) = \arg \min_{\gamma_e \in [0,1]} TCO(\alpha^*, T_{year}, \gamma_e) \quad (40)$$

Since this problem has one decision variable, we employ a grid-based method to determine  $\gamma_e^*$ . The analysis of the optimal solution to this problem, depicted in Fig. 17, can be divided into multiple regions:

- if the tractor operates with high loads ( $\alpha^* > 0.6$ ), then it is economically attractive to use hybrid powertrains with low electrification ratios ( $\gamma_e^* \rightarrow 0$ ), i.e., with small electric motor and battery.

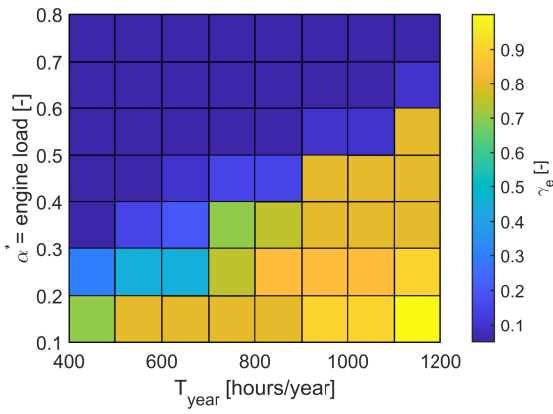


Fig. 17. Representation of the best electrification ratio  $\gamma^*$  for different operating conditions.

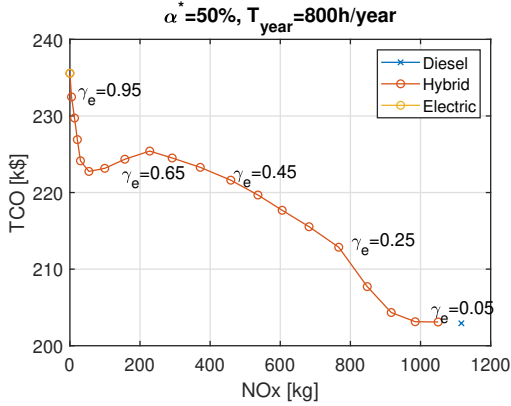


Fig. 18. Impact of electrification ratio ( $\gamma_e$ ) in total lifetime NOx emissions and TCO.

- for low loads ( $\alpha^* < 0.2$ ) the best electrification ratio approaches 1. In this case, the tractor is mostly "electric" and uses a small diesel engine to extend its operation range at a low cost.
- for intermediate loads ( $\alpha^* \in (0.2, 0.6)$ ) there is a transition zone where the electrification ratio switches from high to low  $\gamma_e$ .

The electrification ratio  $\gamma_e$  also plays a vital role in the tractor emissions. Fig. 18 provides a trade-off analysis between TCO and NOx emissions for an average load  $\alpha^* = 0.5$  and  $T_{year} = 800\text{h/year}$ , while varying the electrification ratio from 0.05 to 0.95. The results reveal that higher values of  $\gamma_e$  lead to a decrease in NOx emissions. For example, an electrification ratio of 0.25 can reduce NOx emissions by 30% while increasing cost by only 5% when compared to diesel powertrains. Further decreases in NOx emissions are possible by increasing  $\gamma_e$  and total costs.

Fig. 19 illustrates the impact of the hybrid powertrain (with  $\gamma_e = 0.25$ ) in the parameter space<sup>6</sup>  $P^*$ . In comparison with electric, the hybrid powertrain significantly expands the affordability area. For example, considering the load  $\alpha = 0.4$ , the hybrid powertrain is more affordable than diesel for operating

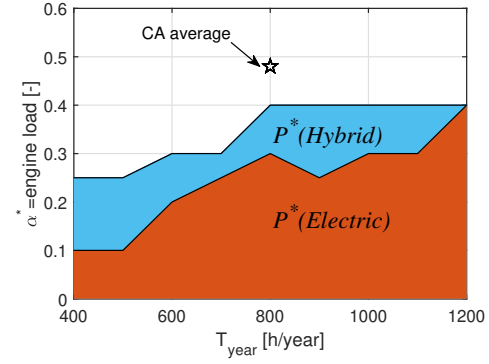


Fig. 19. Sensitivity analysis of the set  $P^*$  for different powetrain types (electric vs hybrid with  $\gamma_e = 0.25$ ). The star mark depicts the average operating conditions of tractors in California (motor load  $\alpha = 0.46$  and  $800\text{h/year}$ ).

times as low as  $800\text{h/year}$ . In contrast, the electric powertrain needs at least  $1200\text{h/year}$  to be economically competitive. It is also interesting to compare the  $\Delta TCO^{d,e}$  and  $\Delta TCO^{d,h}$  (see Fig. 13(b)). The results show the economic savings offered by an electric powertrain surpasses the ones obtained with a hybrid tractor for low loads, i.e.,  $\Delta TCO^{d,h} > \Delta TCO^{d,e}$ . The hybrid powertrain is better suited to tackle high loads.

Fig. 23 included in Appendix B depicts the cost breakdown for  $\alpha^* = 0.6$ . While electric is slightly more expensive than hybrid when  $T_{year} = 400\text{h/year}$ , the situation is reversed for higher usage times. At  $T_{year} = 1200\text{h/year}$ , the total cost of ownership of a hybrid tractor is 12% lower than that of an electric (but 2.7% more expensive than diesel).

#### G. Estimating subsidies for adoption of electric tractors

The TCO tool developed in this work can also help policymakers quantify the value of subsidies needed to stimulate the adoption of electrified tractors. More specifically, policymakers can use the outputs of our models,  $\Delta TCO^{d,e}$  (and  $\Delta TCO^{d,h}$ ), to estimate the subsidy amount that farmers could receive to offset the additional acquisition costs of electrified tractors. This estimate will depend on the expected tractor load and annual working time in the region where the subsidy is applied. Let us consider California as an example. The average engine load and average annual working time in this state is [64]:

$$\alpha_{CA} = 0.48, \quad T_{year,CA} = 800\text{h/year} \quad (41)$$

Under these average operating conditions, the amount of subsidy could be set as:

$$\Delta TCO^{d,e}(\alpha_{CA}, T_{year,CA}) \approx \$21.5k \quad (42)$$

$$\Delta TCO^{d,h}(\alpha_{CA}, T_{year,CA}) \approx \$4.5k \quad (43)$$

These estimates were computed based on the results present in Fig. 13(a) and 13(b).

#### H. Stochastic Analysis

Up to now, the TCO results have been analyzed with a deterministic framework. In this section, we will treat the

<sup>6</sup>In this case, we make use of the TCO difference between diesel and hybrid powertrain  $P^* = \{p : \Delta TCO^{d,h}(p) > 0\}$

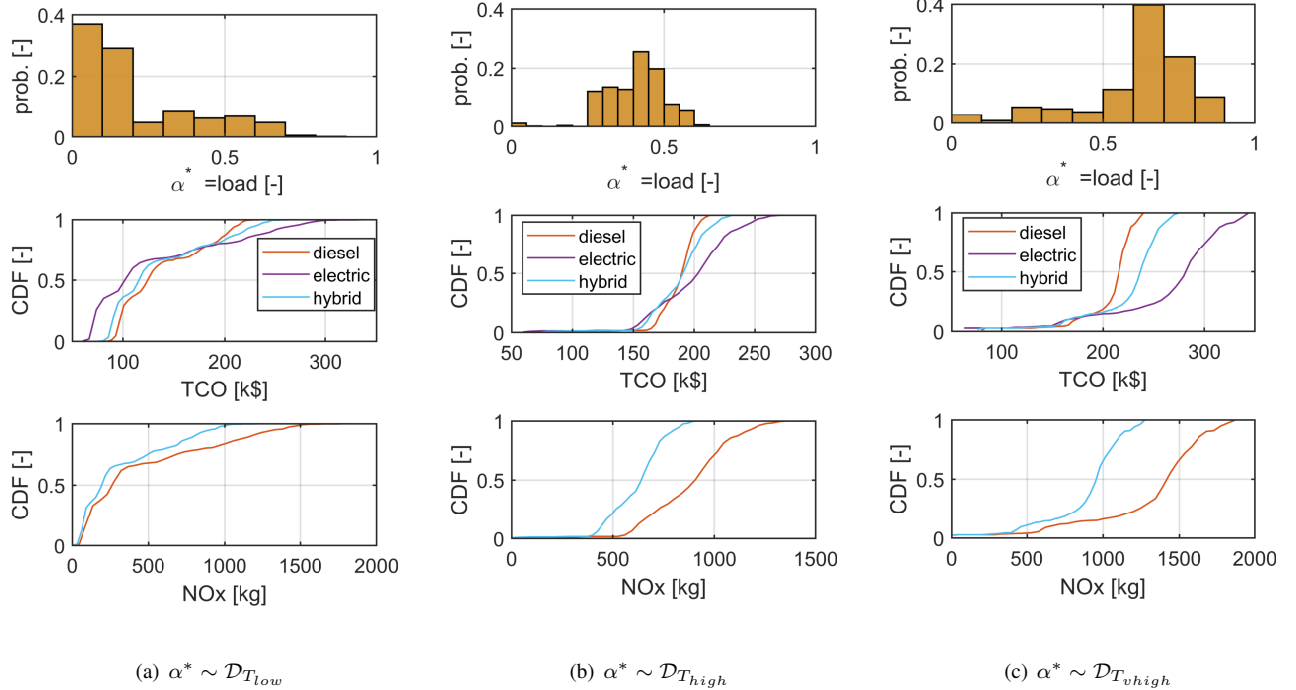


Fig. 20. Stochastic analysis of the TCO of electric, diesel and hybrid ( $\gamma_e = 0.25$ ) tractors for low (a), high (b) and very high(c) tractor loads. Note: top row of plots depict the probability distribution of tractor load; the last two rows illustrate the cumulative distribution function for the TCO and NOx emission. We consider working time per year = 800h/year.

TABLE V  
MEAN AND STANDARD DEVIATION OF TCO AND NOX EMISSIONS  
CONSIDERING DIFFERENT ENGINE LOADS AND POWERTRAINS.

| Load        | Powertrain | TCO    |                    | NOx    |                    |
|-------------|------------|--------|--------------------|--------|--------------------|
|             |            | Mean   | Standard Deviation | Mean   | Standard Deviation |
| $T_{low}$   | Diesel     | \$139k | \$39k              | 449kg  | 383kg              |
|             | Electric   | \$130k | \$61k              | 0kg    | 0kg                |
|             | Hybrid     | \$135k | \$45k              | 317kg  | 262kg              |
| $T_{med}$   | Diesel     | \$181k | \$25k              | 820kg  | 317kg              |
|             | Electric   | \$190k | \$49k              | 0kg    | 0kg                |
|             | Hybrid     | \$181k | \$34k              | 575kg  | 210kg              |
| $T_{high}$  | Diesel     | \$191k | \$17k              | 936kg  | 221kg              |
|             | Electric   | \$208k | \$34k              | 0kg    | 0kg                |
|             | Hybrid     | \$194k | \$23k              | 654kg  | 144kg              |
| $T_{vhigh}$ | Diesel     | \$213k | \$27k              | 1382kg | 385kg              |
|             | Electric   | \$275k | \$58k              | 0kg    | 0kg                |
|             | Hybrid     | \$232k | \$37k              | 938kg  | 256kg              |

engine  $\alpha^*$  as a random variable and investigate its impact on the TCO and lifetime NOx emissions of the tractor using the following stochastic framework:

$$TCO^j(\alpha^*), \quad m_{NOx}^j(\alpha^*), \quad \alpha^* \sim \mathcal{D}_k \quad (44)$$

where  $j \in \{e, d, h\}$  and  $\alpha^*$  is a stochastic variable with probabilistic distribution  $\mathcal{D}_k$ . This distribution is computed based on the experimental data of the four tractors discussed in Section II-B. Four probability distributions are considered:

- *low load*, from tractor  $k = T_{low}$
- *medium load*, from tractor  $k = T_{med}$
- *high load*, from tractor  $k = T_{high}$
- *very high load*, from tractor  $k = T_{vhigh}$ .

A Monte Carlo simulation method is employed to compute the resulting probabilistic distributions of  $TCO^j$  and  $m_{NOx}^j(\alpha^*)$ , where  $\alpha^*$  is sampled from  $\mathcal{D}_k$ . Fig. 20 provides the probability distribution of TCO and NOx for different engine load profiles  $\mathcal{D}_k$ .

*Low load case* ( $\mathcal{D}_{T_{low}}$ ) is depicted in Fig. 20a. The distribution of this engine load is skewed with a peak at around  $\alpha = 0.1$  and a long tail on the right side. The cumulative distribution function (CDF) of the TCO also provides useful insights. For example, the probability( $TCO(electric) < TCO(diesel)$ ) = 70%. On average, the hybrid powertrain reduces NOx emissions in 30% when compared to diesel (see Table V and Fig. 21).

*High load case* ( $\mathcal{D}_{T_{high}}$ ) is depicted in Fig. 20b. The distribution of engine load is approximately symmetrical, with a peak at around  $\alpha = 0.4$ . The diesel and hybrid tractor have similar average TCO values (close to 190k), while the electric is more expensive. Here, it is worth noticing that the variance of the TCO (electric) and TCO (hybrid) is significantly higher than TCO(diesel) – Table V shows an increase in 100% in standard variation. We hypothesize that this higher variance is due to the additional cost components in the electric and hybrid powertrain (e.g., battery + infrastructure costs), leading to the higher cost spread. The hybrid powertrain is also capable of significantly reducing the NOx emissions. A closer inspection of the distribution of NOx emissions reveals that most of the emissions for the hybrid powertrain are concentrated in the range of 400 to 900kg, while the diesel ranges from 500kg to 1300kg.

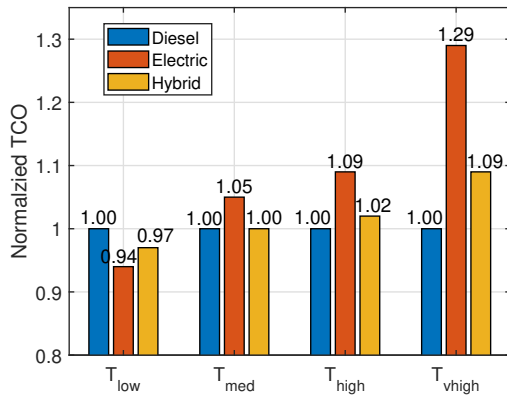


Fig. 21. Representation of the mean TCO for different engine load profiles ( $T_{low}$ ,  $T_{med}$ ,  $T_{high}$ ,  $T_{vhigh}$ ) and powertrains (diesel, electric, hybrid). Note: all results are normalized with respect to the Diesel powertrain.

The analysis of the *medium load case* ( $\mathcal{D}_{T_{med}}$ ), depicted in Fig. 21, reveals that the TCO of this case falls between the TCO of  $T_{low}$  and  $T_{high}$ . Since the trend of  $T_{med}$  is aligned with the other load cases, we decided to omit the detailed probabilistic distribution of  $T_{med}$  for the sake of brevity.

*Very high load case* ( $\mathcal{D}_{T_{vhigh}}$ ): This scenario has an engine load distribution with a peak around 0.65 and a long tail on the left side. The CDF of the total cost shows that the diesel powertrain is the most affordable option in 80% of the cases. Diesel powertrains provide more affordable TCO. On average, diesel is 9% cheaper than hybrid and 28% cheaper than electric (see Fig. 21a). However, they also generate 32% higher emissions than the hybrid powertrains (see Table V). This scenario with heavy loads is the most difficult for cost-effective electrification.

## V. CONCLUSION AND OUTLOOK

This work presented a techno-economic study to identify favorable operating conditions for deploying electric and hybrid tractors. We developed pragmatic simulation models to predict energy consumption and emissions of the tractors and sizing guidelines to define battery capacity and charging power. A model predictive controller was also proposed to manage energy in the hybrid powertrain. An economic model was then employed to estimate the total costs of ownership of tractors, considering acquisition, infrastructure, energy and maintenance costs. A realistic use case based on experimental data collected from tractors in a California farm was employed to compare the costs of the different powertrains. We concluded that:

- For light-duty tasks characterized by engine loads inferior to 20%, the electric tractor is an attractive option. Electric powertrains can reduce by up to 19% the total cost of ownership compared to diesel powertrains while offering zero local emissions.
- For medium-duty tasks, where the engine load varies between 30% and 60%, hybrid powertrains provide a promising path. In these conditions, hybrid shows similar total costs as diesel powertrains but can reduce NOx emissions by up to 30%.

- For heavy-duty farm operations, where the engine load exceeds 60%, it isn't easy to electrify the tractor at an affordable cost.

We expect the results generated in this work to be useful for farmers, policymakers and engineers currently planning electrification of farming fleets. For farmers, this techno-economic study can help them select the most affordable powertrain for their use case. The low-dimension decision maps created in this work (Fig. 15) require only average engine load and annual working time, variables farmers can easily estimate (e.g. via telematic software onboard existing tractors). These maps help farmers quickly determine if electric tractors are economically viable, and can be used in outreach activities to encourage adoption of clean powertrains in agriculture. For policymakers, this study can be used to quantify the economic incentives needed to offset the higher acquisition costs of electric tractors. For engineers, our study provides a systematic methodology that they can use for sizing and analyzing total ownership costs, energy efficiency, and emissions of electrified powertrains.

In future developments of our techno-economic tool, we plan to consider installation and operation costs of onsite renewable energy sources, such as solar, wind, and biogas. This locally-generated renewable energy could be used to charge electric tractors or be sold to the grid, providing an additional revenue stream for farmers. Onsite energy generation could also facilitate the electrification of large farming fleets, which may require significant charging power that the grid is currently unable to deliver in remotely-located farms.

## DECLARATION OF GENERATIVE AI AND AI-ASSISTED TECHNOLOGIES IN THE WRITING PROCESS

During the preparation of this work, the authors used ChatGPT to rectify grammatical errors and improve the readability of the text. After using this tool, the authors reviewed and edited the content as needed and take full responsibility for the content of the publication.

## APPENDIX

### A. Parameters of the NO<sub>x</sub> Emission Model

Fig. 22 provides the values of the zero-emission factor ( $EF_0$ ) and deterioration rate  $EF_{DR}$  of the NO<sub>x</sub> emission model employed in this work.

### B. Supplementary Results for Hybrid Powertrain

Fig. 23 depicts the cost breakdown of TCO for diesel, electric, and hybrid powertrains for a high engine load ( $\alpha^* = 0.6$ ).

## REFERENCES

- [1] M. Gonzalez-de Soto, L. Emmi, C. Benavides, I. Garcia, and P. Gonzalez-de Santos, "Reducing air pollution with hybrid-powered robotic tractors for precision agriculture," *Biosystems Eng.*, vol. 143, pp. 79–94, Mar. 2016.
- [2] "The world bank," <https://data.worldbank.org/indicator/AG.AGR.TRAC.NO>, accessed: 2022-11-18.

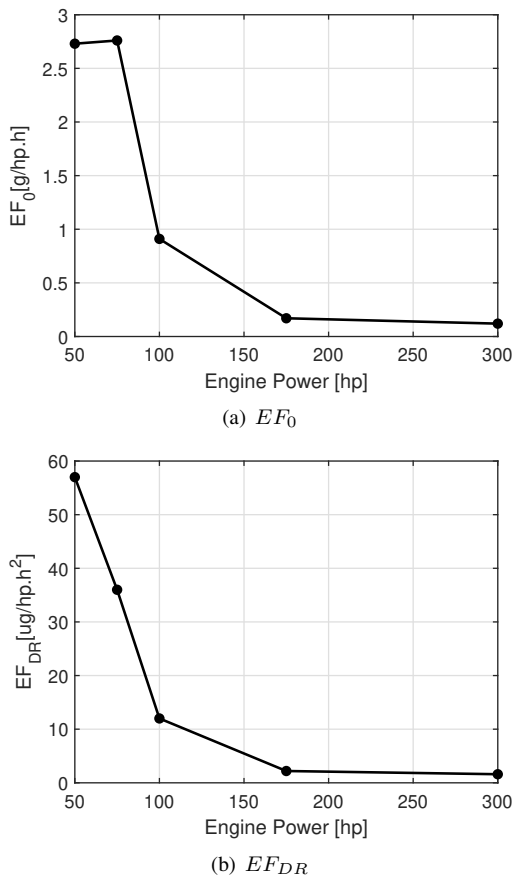


Fig. 22. Graphical representation of the parameters of the NOx emission model, including a) the zero-hour emission factor ( $EF_0$ ) and ii) deterioration rate ( $EF_{DR}$ ) as function of the engine's nominal power. The value for these parameters was extracted from [50], considering year 2023 and a fuel correction factor  $FCF = 0.95$ .

- [3] Executive Department, State of California, "Executive order N-79-20," <https://www.gov.ca.gov/wp-content/uploads/2020/09/N.23-20-EO-N-79-20-Climate.pdf>, accessed: 2023-2-19.
- [4] "Monarch tractors," <https://www.monarchtractor.com/>, accessed: 2022-11-18.
- [5] "Solectrac," <https://solectrac.com/>, accessed: 2022-11-18.
- [6] M. M. Rahman, I. Khan, D. L. Field, K. Techato, and K. Alameh, "Powering agriculture: Present status, future potential, and challenges of renewable energy applications," *Renewable Energy*, vol. 188, pp. 731–749, Apr. 2022.
- [7] R. M. Babu, M. S, and N. R. P, "Electrical operated fan for cooling system on agricultural tractors," in *SAE Technical Paper Series*, no. 2019-26-0079. 400 Commonwealth Drive, Warrendale, PA, United States: SAE International, Jan. 2019.
- [8] E. Scolaro, M. Beligoj, M. P. Estevez, L. Alberti, M. Renzi, and M. Mattetti, "Electrification of agricultural machinery: A review," *IEEE Access*, vol. 9, pp. 164 520–164 541, 2021.
- [9] N.-L. Vu, P. Messier, B.-H. Nguyn, T. Vo-Duy, J. P. F. Trovão, A. Desrochers, and A. Rodrigues, "Energy-optimization design and management strategy for hybrid electric non-road mobile machinery: A case study of snowblower," *Energy*, vol. 284, p. 129249, Dec. 2023.
- [10] F. Mocera and A. Somà, "Analysis of a parallel hybrid electric tractor for agricultural applications," *Energies*, vol. 13, no. 12, p. 3055, Jun. 2020.
- [11] M. Beligoj, E. Scolaro, L. Alberti, M. Renzi, and M. Mattetti, "Feasibility evaluation of hybrid electric agricultural tractors based on life cycle cost analysis," *IEEE Access*, vol. 10, pp. 28 853–28 867, 2022.
- [12] F. Un-Noor, G. Wu, H. Perugu, S. Collier, S. Yoon, M. Barth, and K. Boriboonsomsin, "Off-Road construction and agricultural equipment electrification: Review, challenges, and opportunities," *Vehicles*, vol. 4, no. 3, pp. 780–807, Aug. 2022.
- [13] M. Ehsani, K. V. Singh, H. O. Bansal, and R. T. Mehrjardi, "State of the art and trends in electric and hybrid electric vehicles," *Proc. IEEE*, vol. 109, no. 6, pp. 967–984, Jun. 2021.
- [14] D. Troncon, L. Alberti, and M. Mattetti, "A feasibility study for agriculture tractors electrification: Duty cycles simulation and consumption comparison," in *2019 IEEE Transportation Electrification Conference and Expo (ITEC)*, Jun. 2019, pp. 1–6.
- [15] A. Lajunen, "Simulation of energy efficiency and performance of electrified powertrains in agricultural tractors," in *2022 IEEE Vehicle Power and Propulsion*, 2022.
- [16] V. Olkkonen, A. Lind, E. Rosenberg, and L. Kvalbein, "Electrification of the agricultural sector in norway in an effort to phase out fossil fuel consumption," *Energy*, vol. 276, p. 127543, 2023.
- [17] A. Desreux, E. Hittinger, A. Bouscayrol, E. Castex, and G. M. Sirbu, "Techno-economic comparison of total cost of ownership of electric and diesel vehicles," *IEEE Access*, vol. 8, pp. 195 752–195 762, 2020.
- [18] A. Burnham, D. Gohlke, L. Rush, T. Stephens, Y. Zhou, M. Delucchi, A. Birk, C. Hunter, Z. Lin, S. Ou, F. Xie, C. Proctor, S. Wiryadinata, N. Liu, and M. Boloor, "Comprehensive total cost of ownership quantification for vehicles with different size classes and powertrains," Argonne National Laboratory (ANL), Tech. Rep., Apr. 2021.
- [19] California Air Resources Board (CARB), "Emissions inventory for agricultural diesel vehicles," Tech. Rep., 2018.
- [20] D. Bochtis, C. A. G. Sorensen, and D. Kateris, *Operations Management in Agriculture*. San Diego, CA: Academic Press, Nov. 2018.
- [21] M. Lips, "Length of operational life and its impact on life-cycle costs of a tractor in switzerland," *Agriculture*, vol. 7, no. 8, p. 68, 2017.
- [22] "Agricultural machinery management data (ASAE 496.2)," 1999.
- [23] O. Lagnelov, S. Dhillon, G. Larsson, D. Nilsson, A. Larsolle, and P.-A. Hansson, "Cost analysis of autonomous battery electric field tractors in agriculture," *Biosystems Eng.*, vol. 204, pp. 358–376, Apr. 2021.
- [24] H. H. Vogt, R. R. de Melo, S. Daher, B. Schmuelling, F. L. M. Antunes, P. A. dos Santos, and D. Albiero, "Electric tractor system for family farming: Increased autonomy and economic feasibility for an energy transition," *Journal of Energy Storage*, vol. 40, p. 102744, 2021.
- [25] Z. Shao and S. Anup, "Incentives for electrifying agricultural tractors in india," 2022.
- [26] X. Lü, S. Li, X. He, C. Xie, S. He, Y. Xu, J. Fang, M. Zhang, and X. Yang, "Hybrid electric vehicles: A review of energy management strategies based on model predictive control," *Journal of Energy Storage*, vol. 56, p. 106112, Dec. 2022.
- [27] A. Lajunen, K. Kivekäs, V. Freyermuth, R. Vijayagopal, and N. Kim, "Simulation-based assessment of energy consumption of alternative powertrains in agricultural tractors," *World Electric Vehicle Journal*, vol. 15, no. 3, p. 86, 2024.
- [28] S. Radrizzani, G. Panzani, L. Trezza, S. Pizzocaro, and S. Savaresi, "An add-on model predictive control strategy for the energy management of hybrid electric tractors," *IEEE Transactions on Vehicular Technology*, 2024.
- [29] G. Curiel-Olivares, S. Johnson, G. Escobar, and R. Schacht-Rodríguez, "Model predictive control-based energy management system for a hybrid electric agricultural tractor," *IEEE Access*, vol. 11, pp. 118 801–118 811, 2023.
- [30] E. Borgonovo and E. Plischke, "Sensitivity analysis: A review of recent advances," *Eur. J. Oper. Res.*, vol. 248, no. 3, pp. 869–887, Feb. 2016.
- [31] O. Lagnelöv, G. Larsson, A. Larsolle, and P.-A. Hansson, "Impact of lowered vehicle weight of electric autonomous tractors in a systems perspective," *Smart agricultural technology*, vol. 4, p. 100156, 2023.
- [32] A. Dilawer, R. de Castro, R. Ehsani, and S. Vougioukas, "Identifying practical pathways for electrification of agricultural vehicles through Techno-Economic analysis," in *36th Electric Vehicle Symposium and Exposition*, 2023.
- [33] K. Theodor Renius, *Fundamentals of Tractor Design*. Springer, 2020.
- [34] California Department of Food and Agriculture (CDFA), "California agricultural statistics review 2022-2023," [https://www.cdfa.ca.gov/Statistics/PDFs/2022-2023\\_california\\_agricultural\\_statistics\\_review.pdf](https://www.cdfa.ca.gov/Statistics/PDFs/2022-2023_california_agricultural_statistics_review.pdf), accessed: 2024-8-12.
- [35] D. Hunt and D. Wilson, *Farm Power and Machinery Management: Eleventh Edition*. Waveland Press, 2015.
- [36] V. Muenzel, J. de Hoog, M. Brazil, A. Vishwanath, and S. Kalyanaraman, "A Multi-Factor battery cycle life prediction methodology for optimal battery management," in *Proceedings of the 2015 ACM Sixth International Conference on Future Energy Systems*, ser. e-Energy '15. New York, NY, USA: Association for Computing Machinery, Jul. 2015, pp. 57–66.
- [37] R. E. Araújo, R. de Castro, C. Pinto, P. Melo, and D. Freitas, "Combined sizing and energy management in EVs with batteries and supercapac-

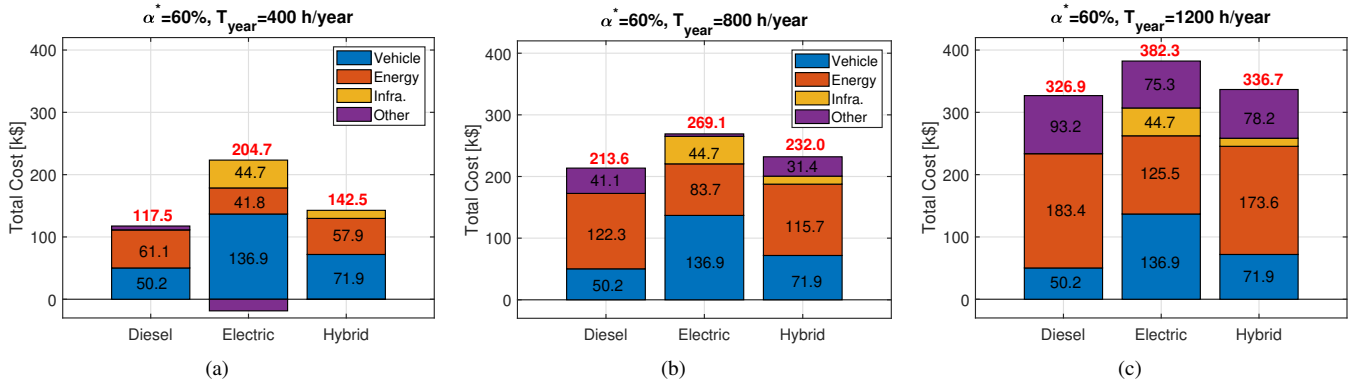


Fig. 23. Cost breakdown of TCO for diesel, electric, and hybrid powertrains.

- itors,” *IEEE Trans. Veh. Technol.*, vol. 63, no. 7, pp. 3062–3076, Sep. 2014.
- [38] M. Xu, R. Wang, B. Reichman, and X. Wang, “Modeling the effect of two-stage fast charging protocol on thermal behavior and charging energy efficiency of lithium-ion batteries,” *Journal of Energy Storage*, vol. 20, pp. 298–309, Dec. 2018.
- [39] A. V. J. S. Praneeth and S. S. Williamson, “A review of front end AC-DC topologies in universal battery charger for electric transportation,” in *2018 IEEE Transportation Electrification Conference and Expo (ITEC)*, Jun. 2018, pp. 293–298.
- [40] F. Zheng, Y. Xing, J. Jiang, B. Sun, J. Kim, and M. Pecht, “Influence of different open circuit voltage tests on state of charge online estimation for lithium-ion batteries,” *Appl. Energy*, vol. 183, pp. 513–525, Dec. 2016.
- [41] A. Gray, “New holland’s emission-free T4 electric power utility tractor,” <https://www.agriculture.com/new-holland-s-t4-electric-power-utility-tractor-7966136>, Sep. 2023, accessed: 2024-8-12.
- [42] F. M. N. U. Khan, M. G. Rasul, A. S. M. Sayem, and N. K. Mandal, “Design and optimization of lithium-ion battery as an efficient energy storage device for electric vehicles: A comprehensive review,” *Journal of Energy Storage*, vol. 71, p. 108033, Nov. 2023.
- [43] “List of Pre-Parameterized components - MATLAB, simulink electrical,” <https://www.mathworks.com/help/sps/ug/pre-parameterized-components.html>, accessed: 2024-8-14.
- [44] “Agricultural machinery management data (ASAE d497.4),” American Society of Agricultural Engineers, Tech. Rep., 1999.
- [45] “NTTL report search,” <https://tractortestlab.unl.edu/test-page-nttl>, accessed: 2024-8-14.
- [46] “Fendt fendt 211 vario gen3: Performance and fuel consumption during field and transport applications,” [https://pruefberichte.dlg.org/filestorage/PowerMix\\_Datenblatt\\_Fendt-211-S-Vario\\_en.pdf](https://pruefberichte.dlg.org/filestorage/PowerMix_Datenblatt_Fendt-211-S-Vario_en.pdf), accessed: 2023-11-NA.
- [47] R. D. Grisso, D. H. Vaughan, and G. T. Roberson, “Fuel prediction for specific tractor models,” *Appl. Eng. Agric.*, vol. 24, no. 4, pp. 423–428, 2008.
- [48] “DLGpowermix dawn of a new tractor testing era,” [https://edisciplinas.usp.br/pluginfile.php/5166566/mod\\_resource/content/0/POWERMIX\\_PROFIL\\_PI\\_010\\_015\\_04\\_06.pdf](https://edisciplinas.usp.br/pluginfile.php/5166566/mod_resource/content/0/POWERMIX_PROFIL_PI_010_015_04_06.pdf), accessed: 2023-11-NA.
- [49] California Air Resources Board (CARB), “2017 Off-Road diesel emission factor update for NOx and PM,” [https://ww2.arb.ca.gov/sites/default/files/classic/msei/ordiesel/ordas\\_ef\\_fcf\\_2017.pdf](https://ww2.arb.ca.gov/sites/default/files/classic/msei/ordiesel/ordas_ef_fcf_2017.pdf), accessed: 2023-11-NA.
- [50] ——, “2017 Off-Road diesel, propane, & gasoline emission factors,” [https://ww2.arb.ca.gov/sites/default/files/2024-05/ordas\\_ef\\_fcf\\_2017\\_v8.xlsx](https://ww2.arb.ca.gov/sites/default/files/2024-05/ordas_ef_fcf_2017_v8.xlsx), accessed: 2024-5-25.
- [51] A. Wächter and L. T. Biegler, “On the implementation of an interior-point filter line-search algorithm for large-scale nonlinear programming,” *Math. Program.*, vol. 106, no. 1, pp. 25–57, Mar. 2006.
- [52] California Air Resources Board (CARB), “Advanced clean fleets total cost of ownership discussion document,” Tech. Rep., 2021.
- [53] “BloombergNEF,” <https://about.bnef.com/blog/lithium-ion-battery-pack-prices-rise-for-first-time-to-an-average-of-151-kwh/>, accessed: 2022-12-13.
- [54] K. Boriboonsomsin, F. Un-Noor, G. Scora, G. Wu, “Hybridization and full electrification potential in Off-Road applications,” CARB, Tech. Rep., 2022.
- [55] “California city, county sales and use tax rates,” <https://www.cdtfa.ca.gov/taxes-and-fees/sales-use-tax-rates.htm>, accessed: 2022-12-13.
- [56] B. Propfe, M. Redelbach, D. J. Santini, and H. Friedrich, “Cost analysis of plug-in hybrid electric vehicles including maintenance & repair costs and resale values,” *World Electric Vehicle Journal*, vol. 5, no. 4, pp. 886–895, Dec. 2012.
- [57] A. König, L. Nicoletti, D. Schröder, S. Wolff, A. Waclaw, and M. Lienkamp, “An overview of parameter and cost for battery electric vehicles,” *World Electr. Veh. J.*, 2021.
- [58] International Council on Clean Transportation, “Estimating electric vehicle charging infrastructure costs across major U.S. metropolitan areas,” Tech. Rep., 2019.
- [59] S. Ray, K. Kasturi, S. Patnaik, and M. R. Nayak, “Review of electric vehicles integration impacts in distribution networks: Placement, charging/discharging strategies, objectives and optimisation models,” *Journal of Energy Storage*, vol. 72, p. 108672, Nov. 2023.
- [60] C. N. A. Rogers, “Reducing EV charging infrastructure costs,” Rocky Mountain Institute, Tech. Rep., 2019.
- [61] U.S. Energy Information Administration, “<https://www.eia.gov/>,” accessed: 2022-11-18.
- [62] M. A. Hannan, S. B. Wali, P. J. Ker, M. S. A. Rahman, M. Mansor, V. K. Ramachandaramurthy, K. M. Muttaqi, T. M. I. Mahlia, and Z. Y. Dong, “Battery energy-storage system: A review of technologies, optimization objectives, constraints, approaches, and outstanding issues,” *Journal of Energy Storage*, vol. 42, p. 103023, Oct. 2021.
- [63] L. Maufer, F. Duffner, W. G. Zeier, and J. Leker, “Battery cost forecasting: a review of methods and results with an outlook to 2050,” *Energy Environ. Sci.*, vol. 14, no. 9, pp. 4712–4739, 2021.
- [64] California Air Resources Board (CARB), “2021 agricultural equipment emission inventory,” Tech. Rep., 2021.